



universität
wien

Diplomarbeit

Titel der Diplomarbeit

Characterization of the potential Tumor Suppressor Gene N33 (TUSC3) in Ovarian Cancer

angestrebter akademischer Grad

Magister der Naturwissenschaften (Mag.rer.nat.)

Verfasser:	Alfred Gugerell
Matrikelnummer:	0100482
Studienrichtung (lt. Studienblatt):	Anthropologie
Betreuerin:	Univ.Prof. MMag Dr. Sylvia Kirchengast

Wien, im Mai 2008

Danksagung

Zuerst möchte ich hier meiner Familie danken, meinen Eltern, dass sie mir meine Ausbildung ermöglicht haben, meinen Geschwistern und Verwandten für die seelische Unterstützung und Begleitung auf meinem bisherigen Lebensweg.

Danke auch an Prof. Dr. Michael Krainer, dass ich in seinem Labor aufgenommen wurde, so viel lernen durfte und bis hierher begleitet und geleitet wurde, Prof. Dr. Sylvia Kirchengast für die Begeisterung für die Anthropologie und Betreuung als Diplomand, Didi, Michi, Michi, Thomas, Jochen und Ahmed für die Engelsgeduld und die Unterstützung bei der manchmal auch frustrierenden Laborarbeit.

Mein besonderer Dank gilt hier aber meinen Freunden, ohne die ich es niemals so weit geschafft hätte. Ob in der Wohnung, auf der Uni, beim Bier oder bei Prüfungen – ob Ratschläge, aufmunternde Worte oder Zusammenarbeit.

Danke Alex, Stefan, Sabrina, Heiße, Betty, Pamela, Martina, Niki, Bea, Verena, Julia, Vero... und wer noch aller eine Schulter zum Anlehnen hatte.

Wer mir aber am meisten Kraft gegeben hat und hinter mir gestanden ist, vor allem im letzten, härtesten Jahr, ist Ruth. Ohne sie hätte ich es nie geschafft. Ob als Arbeitskollegin, Freundin oder Lebenspartnerin – Danke!

Zum Schluss möchte ich meinen Fans danken.

„Das Leben ist wert, gelebt zu werden, sagt die Kunst, die schönste Verführerin;
das Leben ist wert, erkannt zu werden, sagt die Wissenschaft.“

Friedrich Nietzsche (1844-1900), dt. Philosoph

Table of Contents

ABSTRACT	5
ZUSAMMENFASSUNG	6
1. INTRODUCTION	7
1.1. The human Ovary.....	7
1.1.1. Physiology:	7
1.1.2. Histology:.....	8
1.2. What is Cancer?.....	8
1.2.1. Self-Sufficiency in Growth Signals	8
1.2.2. Insensitivity in Growth-Inhibitory (Antigrowth) Signals – Permanent Proliferation	9
1.2.3. Evading Apoptosis	10
1.2.4. Limitless Replicative Potential	10
1.2.5. Sustained Angiogenesis	11
1.2.6. Tissue Invasion and Metastasis.....	11
1.3. Ovarian Cancer.....	12
1.3.1. Main Types of Ovarian Cancer.....	12
1.3.2. Staging and Grading	14
1.3.3. Risk Factors and Causes for Epithelial Ovarian Cancer	15
1.4. TGF β -Signalling in Normal OSE and Ovarian Carcinomas	17
1.5. EMT in Ovarian Tumor Progression.....	17
1.6. TUSC3 / N33.....	19
1.7. Glycosylation and Cancer	20
2. METHODS	22
2.1. Establishing of cell line models	22
2.2. RNA-Isolation	24
2.3. cDNA Synthesis.....	24
2.4. Quantitative Real Time RT-PCR	25
2.5. Protein extraction	25
2.6. Western Blot.....	25
Electrophoresis.....	25
Electro blotting	26
Incubation with antibodies	26
Detection	27
Stripping	27
Buffer composition	27
Sub-cellular fractionation.....	28

2.7. Proliferation	29
2.8. Apoptosis Assay	29
2.9. Adhesion Assay	30
2.10. Migration and Invasion Assays.....	30
Chick chorioallantoic membrane (CAM) Invasion Assay	31
2.11. Immunocytochemical and immunohistochemical staining	31
2.12. Statistical analysis	32
3. RESULTS	34
3.1. Present Results:.....	34
3.2. Establishing of cell line models and TUSC3 expression	37
3.3. Morphology	37
3.4. Proliferation	39
3.5. Apoptosis	40
3.6. Migration and Invasion Assays	41
Chick chorioallantoic membrane (CAM) Invasion Assay	42
3.7. Localization of TUSC3	42
Western blot - Sub-cellular fractionation.....	42
Immunofluorescence.....	43
3.8. Impact on Glycosylation.....	44
3.9. Adhesion Assay	46
4. DISCUSSION	49
4.1. Clinical results and Methylation.....	49
4.2. TUSC3 – Ostp3	50
4.3. In vitro cell line models	50
4.4. Glycosylation	51
4.5. Additional clinical Syndroms: Does N33 play a Role in Mental Retardation?.....	52
5. REFERENCES	54
6. ABBREVIATIONS	57
CURRICULUM VITAE	59

Abstract

Treatment decisions in ovarian cancer are based on tumor stage, grade, and residual tumor after primary debulking surgery. Early diagnosis represents a major challenge and more than three quarters of cases are diagnosed in late stages (FIGO III and IV), molecular markers for early detection and prognosis do not really exist in clinical practice.

By using a systematic screening approach on 8p22, *TUSC3* was found to be significantly down-regulated in ovarian cancer tissues and of potential prognostic value. High homology of *TUSC3* with *OST3*, a subunit of the oligosaccharyltransferase complex in *Saccharomyces cerevisiae*, lets suggest that *TUSC3* is involved in N-glycosylation of proteins. It is well known that alterations of the sugar chain structures of glycoproteins have been found in various tumors.

The subject of this assignment was to investigate the function of *TUSC3* in ovarian cancer. Reconstitution and genetically silencing of *TUSC3 in vitro* was used for sub-cellular localization, functional analysis such as proliferation, apoptosis, adhesion, migration, and invasion, and for exploration of altered N-glycosylation patterns.

TUSC3 expression was significantly down-regulated by epigenetic methylation in ovarian cancer samples compared to controls. Reconstitution of *TUSC3* expression *in vitro* demonstrated its localization to the endoplasmic reticulum as expected from the function of OST3p, its homologue in yeast, which is part of the oligosaccharyltransferase complex. Distinct phenotypical changes, decreased proliferation and increased migration of ovarian cancer cells and altered N-glycosylation pattern of integrin $\beta 1$, resulting in decreased adhesion to collagen I were observed after reconstitution.

In ovarian cancer down-regulation of *TUSC3* is a frequent event and is primarily caused by an epigenetic mechanism. For the first time we show that a gene involved in N-glycosylation of proteins acts as a tumor suppressor gene with strong and independent impact on ovarian cancer patient outcomes.

Zusammenfassung

Entscheidungen zur Behandlung von Eierstockkrebs basieren auf dessen Stadium, Grad und zurückbleibendem Tumor nach chirurgischer Entfernung (cytoreduktive Operation). Die frühzeitige Erkennung stellt eine große Herausforderung dar und mehr als drei Viertel aller Fälle werden in fortgeschrittenen Stadien diagnostiziert (FIGO III und IV), eben auch, da bislang keine molekularen Marker für eine frühe Detektion in klinischer Anwendung existieren.

Bei einem systematischen Screening des Chromosomenabschnitts 8p22 wurde das Gen *TUSC3* in Gewebe von Eierstockkrebs signifikant downreguliert gefunden und hat daher potentiellen prognostischen Wert. Eine hohe Homologie zu *OST3*, eine Untereinheit des Oligosaccharyltransferase-Komplexes in *Saccharomyces cerevisiae* lässt vermuten, dass *TUSC3* in der N-Glycosylierung von Proteinen involviert ist. Es ist wohl bekannt, dass Veränderungen der Zuckerkettenstrukturen von Glycoproteinen in verschiedenen Tumorarten auftauchen.

Der Gegenstand dieser Arbeit war die Untersuchung der Funktion von *TUSC3* in Eierstockkrebs. Zelllinien mit rekonstituiertem, bzw. genetisch gesilenctem *TUSC3* wurden verwendet für innerzelluläre Lokalisation, funktionelle Analysen wie Proliferation, Apoptose, Adhesion, Migration und Invasion, sowie für die Untersuchung von unterschiedlichen N-Glycosylierungsmustern.

Die Expression von *TUSC3* war signifikant downreguliert durch epigenetische Methylierung in Proben von Eierstockkrebs in Bezug zu Kontrollen. Die Rekonstituierung von *TUSC3 in vitro* zeigte dessen Lokalisierung wie erwartet im endoplasmatischen Retikulum, analog zur Funktion von OST3p. Änderungen im Phaenotypus, erhöhte Proliferation und verminderte Migration von Eierstockkrebszellen und veränderte N-Glycosylierungsmuster von Integrin $\beta 1$ und dadurch erhöhte Adhesion zu Collagen I wurden nach der Rekonstitution beobachtet.

Downregulierung von *TUSC3* ist ein häufiges Ereignis bei Eierstockkrebs und in erster Linie durch epigenetische Merkmale bestimmt. Für das erste Mal wurde in diesem Labor gezeigt, dass ein Gen, das in die N-glycosylierung involviert ist, als Tumorsuppressorgen wirkt mit starkem und unabhängigem Einfluss auf das Überleben von Patienten mit Eierstockkrebs.

1. Introduction

1.1. The human Ovary

The ovary is an egg-producing reproductive organ. In human it exists in pairs as a part of the reproductive system in female and measures 2-4 cm in diameter. It is located at the lateral wall of the pelvis (in the ovarian fossa) on either side of the uterus, connected to it by the ovarian ligament [1].

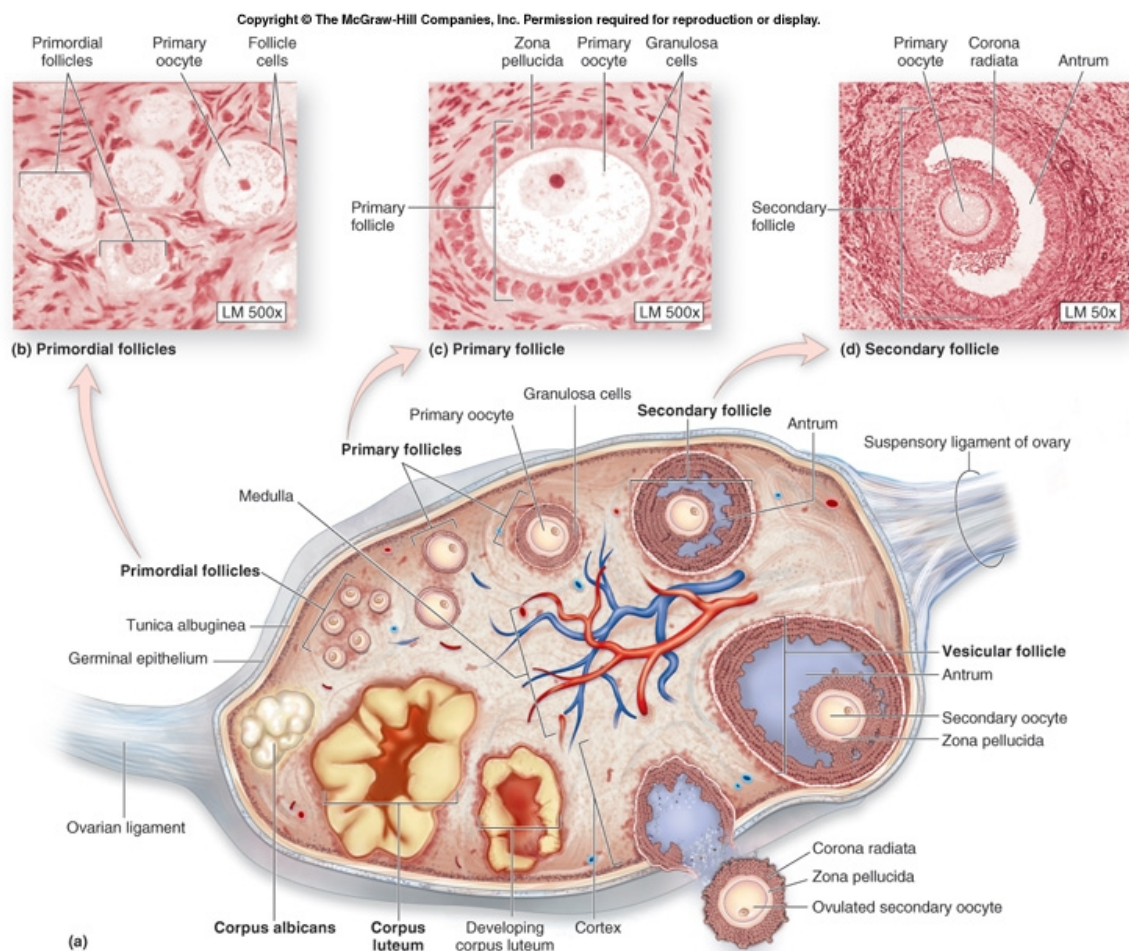


Figure 1 Human ovary, Anatomy and Histology (Kellogg Community College)

1.1.1. Physiology:

The ovaries have two major functions in the female body: an exocrine function (production of eggs) and an endocrine function (hormone secretion – steroid and peptide hormones). The most important hormones are estrogen and progesterone, which play a leading role in puberty (physical changes and building of secondary sex characteristics).

They are responsible for maturation of the uterine endometrium, which ensures the implantation of a fertilized egg. Furthermore, these hormones help maintain the menstrual cycle and are very important players in the brain-pituitary-gonad axis [1].

1.1.2. Histology:

The surface of the ovary is covered by a single layer of cuboidal epithelium, the germinal epithelium, which is the continuation of the peritoneum. Fibrous connective tissue forms a thin capsule, the tunica albuginea, immediately beneath the epithelium, covering the ovarian cortex.

The ovary is divided into an outer cortex and an inner medulla. The cortex consists of a very cellular connective tissue stroma (produces most of the hormones of the ovary) in which the ovarian follicles are embedded. The medulla is composed of loose connective tissue, which contains blood vessels and nerves.

1.2. What is Cancer?

Cells in normal tissue are largely instructed to growth by their neighbours (paracrine signals) or via systemic (endocrine) signals. Cancer cells have defects in regulatory circuits that govern normal cell proliferation and homeostasis. Tumorigenesis in humans is a multistep process where genetic alterations conduct normal cells into highly malignant cells. This is a complex way from normality via series of premalignant states into invasive cancers. Tumor cells are altered at multiple sites having suffered disruption through lesions - e.g. point mutations or obvious things like changes in chromosome complement. According to Hanahan and Weinberg, there are six essential alterations in cell physiology that collectively dictate malignant growth (Fig. 3): [2]

1.2.1. Self-Sufficiency in Growth Signals

Normal cells require mitogenic growth signals (GS) such as growth factors, extracellular matrix components, and cell-to-cell adhesion/interaction molecules, before they can move from a quiescent state into an active proliferative state. Oncogenes act by mimicking these normal growth signals. Thereby, tumor cells generate many of their own growth signals to become independent of stimulation of their normal tissue microenvironment. Three common molecular strategies for gaining autonomy are evident: alteration of extracellular

growth signals (autocrine stimulation, e.g. PDGF and TGF α by glioblastoma), of transcellular transducers of those signals (e.g. EGF-R/erbB and HER2/neu in mammarian carcinoma), or of intracellular circuits that translate those signals into action like the SOS-Ras-Raf-MAP kinase mitogenic cascade.

Many of the growth signals arise from the stromal cell components (not only from the tumor tissue), in which cancer cells have subverted normal cell types to serve as active collaborators for assistance.

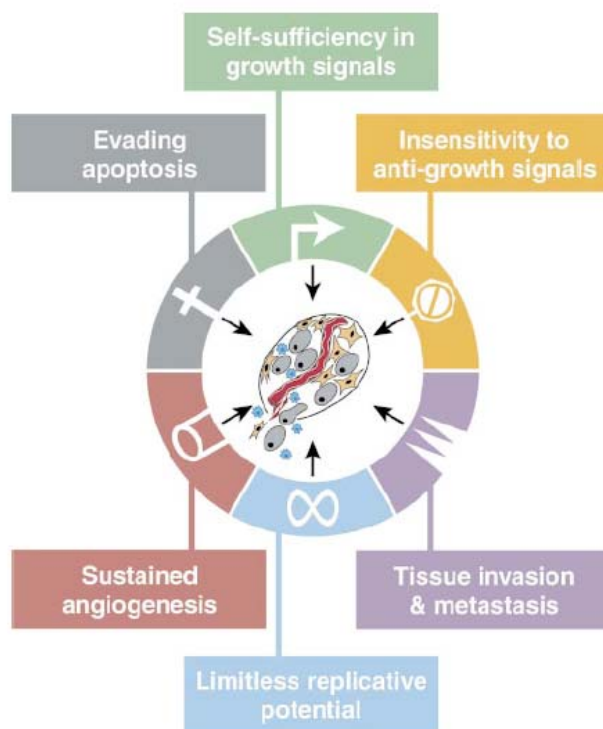


Figure 2 Hallmarks of Cancer (Hanahan & Weinberg)

1.2.2. Insensitivity in Growth-Inhibitory (Antigrowth) Signals – Permanent Proliferation

Within a normal tissue, multiple anti-proliferative signals operate to manage cellular quiescence and tissue homeostasis. Proliferation can be inhibited by antigrowth signals by two distinct mechanisms: Cells may be forced out of the active proliferation cycle into the quiescent state (G_0), of which they can re-emerge when extracellular signs permit. Or cells can be induced to permanent abandon their proliferation potential by entering postmitotic states. Cancer cells must escape these anti-proliferative signals, which are funnelled through the retinoblastoma protein (pRb) and its two relatives, p107 and p130.

1.2.3. Evading Apoptosis

Resistance to apoptosis (the programmed cell death) is among increased proliferation a possibility for tumor cells to expand in number. Apoptosis is a delicate homeostasis with precisely choreographed series of steps which ensures an adequate architectural configuration of cells in a tissue. The cell has sensors and effectors to regulate these pathways: sensors are responsible for observing the extra- and intracellular environment for conditions which decide if a cell should live or die. The effectors are the second type of modulators including cell surface receptors that bind survival or death factors (e.g. survival signals IGF-1/IGF-2 and their receptor EGF-1R, death signals such as FAS ligand and its FAS receptor and TNF α binding to TNF-R1). Besides, the life of most cells is partly kept by cell-cell and cell-matrix adherence-based survival signals.

Many of the signals that activate apoptosis get together on the mitochondria. Pro-apoptotic proteins of the Bcl-2 family such as Bax, Bak, Bid or Bim or with an anti-apoptotic function like Bcl-2, Bcl-XL or Bcl-W act in part by arranging mitochondrial death signalling through cytochrome C release. FAS or cytochrome C activate caspase-8 and -9, intracellular proteases which are the ultimate effectors of apoptosis. These caspases trigger the activation of several effector caspases that perform the death program through selective destruction of subcellular structures and organelles and finally of the genome.

A cancer cell can evade apoptosis by overexpressing an oncogene. The resistance to apoptosis can be acquired by cancer cells through a variety of strategies but the most commonly occurring route involves the *p53* tumor suppressor gene. The PI3 kinase-AKT/PKB pathway, which transmits anti-apoptotic survival signals, often is disturbed too.

1.2.4. Limitless Replicative Potential

Many types of mammalian cells carry a specific, cell-autonomous program that limits their proliferation. This scheme must be disrupted so that a cell can expand to form a macroscopic, life-threatening tumor. Once cell populations have progressed through a certain number of doublings, they stop growing, a progress called senescence. Normal human cell types have the capacity for 60-70 doublings: telomeres, which are composed of several thousand repeats of a short 6 bp sequence element, are the ends of chromosomes which do not code for any gene and protect the ends of chromosomal DNA. This is necessary because of the inability of DNA polymerase to completely replicate the 3' ends of chromosomal DNA during each S phase. 50-100 bp of telomeric DNA drop

away during each cell cycle. Exposed chromosomes tend to build end-to-end fusions, yielding the karyotypic disarray associated with crisis and resulting in the death of the affected cell.

Telomere maintenance is evident in all types of malignant cells, doing so by upregulating expression of the telomerase enzyme, which adds hexanucleotide repeats onto the ends of telomeric DNA, or by activating of ALT, a mechanism which protects and rebuilds the telomeres by recombination-based inter-chromosomal exchanges of sequence information.

1.2.5. Sustained Angiogenesis

The oxygen and nutrients provided by the vasculature are fundamental for cell function and survival, every cell of a tissue must be within 100 μm of a capillary blood vessel. During organogenesis, this proximity is ensured by coordinated growth of vessels and parenchyma. Once a tissue is formed, the growth of new blood vessels (angiogenesis) is transitory and carefully regulated. If a tissue or an organ grows to a larger size, incipient neoplasias must develop angiogenic ability. Vascular endothelial growth factor VEGF and acidic and basic fibroblast growth factors (FGF1/2) are such angiogenesis-initiating signals. Integrin signalling administers to this regulatory balance too. Induction of angiogenesis occurs as an early to midstage event in many human cancers.

1.2.6. Tissue Invasion and Metastasis

In every type of cancer, sooner or later when the primary tumor mass is big enough, it will generate pioneer cells that spread out, invade adjacent tissues, and travel to distant tissues and organs where they may achieve success in founding new colonies. They will colonize new territory where nutrients and space are not a limiting factor. These metastases are the cause of 90% of human cancer deaths. The genetic and biochemical determinants for this event remain incompletely understood.

Several classes of proteins are involved to tie the cells to their surroundings, including cell-cell adhesion molecules (CAMs), which belong to the family of immunoglobulin and cadherins, and integrins, which link cells to extracellular matrix substrates. Best observed in cancer is E-cadherin, a cell-to-cell interaction molecule expressed on epithelial cells. Its function is apparently lost in a majority of epithelial cancers.

The activation of extracellular proteases and the altered binding specificities of cadherins, CAMs, and integrins play a crucial role in achieving invasiveness and metastatic ability, but seem to differ from one tissue environment to another.

1.3. Ovarian Cancer

Ovarian cancer is a malignant tumor on or within an ovary. It is the most lethal gynecologic malignancy and with about six percent the fourth most frequent cause of cancer related death of women in western countries. Estimates indicate that one in 70 women will develop ovarian cancer in her lifetime, with a median survival rate of 4.5 years. A recent cancer statistic reported an estimated 22,200 new cases and 16,210 deaths per year in the United States [3].

Two fundamental reasons explain its aggressive behaviour: most patients are diagnosed with ovarian cancer in an advanced stage, and die of recurrences from disease that has become resistant to conventional chemotherapies. Due to the relative lack of specific signs and symptoms of this disease in the beginning and the lack of effective screening programs, epithelial ovarian cancer is diagnosed at advanced stages in most patients, contributing to low overall cure rates [4]. Early diagnosis represents a major challenge and more than three quarters of cases are diagnosed in late stages (FIGO III and IV). All of these patients need multimodality therapy consisting of optimal debulking surgery and chemotherapy.

Currently accepted prognostic markers include initial staging, grading and size of residual disease after initial cytoreductive surgery [5]. Molecular markers for early detection and prognosis in addition to Cancer Antigen 125 (CA-125) [6] do not exist in clinical practice [7]. Promoter methylation of tumor suppressor genes (TSGs) shows promise as molecular marker. It can deliver insight into the biology of a tumor and in contrast to gene or protein expression it can be detected easily by PCR based methods not only out of tumor material but also in body fluids [8].

1.3.1. Main Types of Ovarian Cancer

Because many ovarian tumors are benign but can become malignant, a broad definition of ovarian cancer includes both, benign and malignant, tumors.

These main types of ovarian cancer can occur:

About 85% to 90% of ovarian cancers are *epithelial ovarian carcinomas* (EOC). Cancerous epithelial tumors are called carcinomas. They have some histological features that can be used to classify the tumor into serous, mucinous, endometrioid, and clear cell types.

Epithelial ovarian tumors (about 85% - 90%):

Benign epithelial ovarian tumors do not spread and usually do not result in a serious illness. This type of epithelial ovarian tumor includes serous adenomas, mucinous adenomas, and Brenner tumors.

Borderline epithelial ovarian cancers are called tumors of low malignant potential (LMP tumors). They do not grow into the ovarian stroma, affects women at a younger age than the typical ovarian cancers, and grow slowly. Although they can be fatal, this is not common.

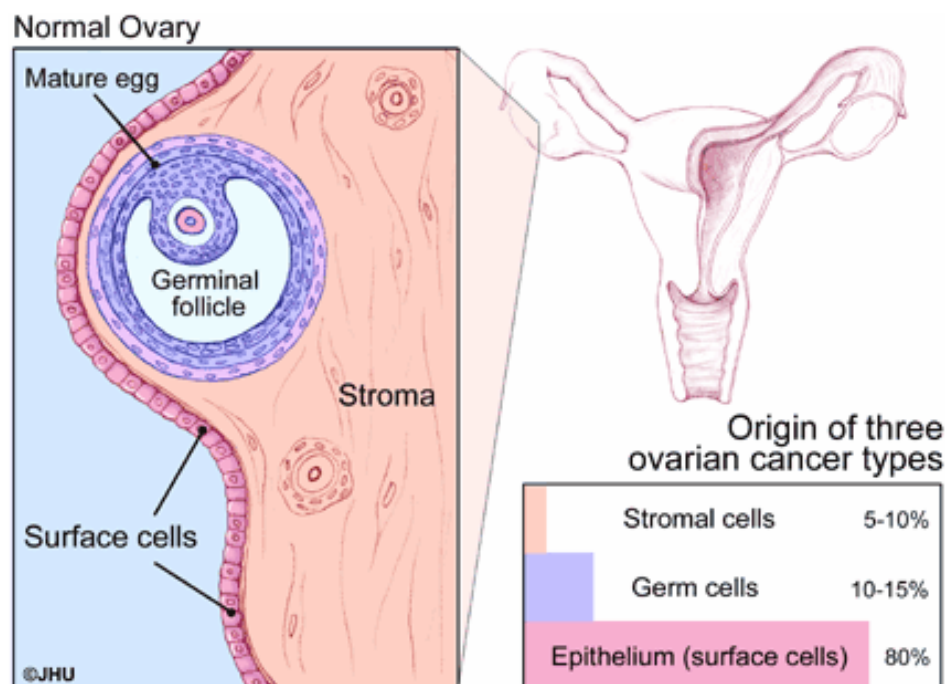


Figure 3 Ovarian Cancer Types (Johns Hopkins University)

Most of the **germ cell tumors** (about 5%) are benign and tend to occur in younger women and girls. They derive from the egg producing cells. Some subtypes are teratomas, dysgerminomas, endodermal sinus tumors, and choriocarcinomas.

Sex cord stromal ovarian tumors (about 8%) derive from connective tissue cells. More than half of the cases with this type are found in women older than 50 years, is rare in comparison to epithelial tumors. Some of these tumors produce estrogen and progesterone, but some also male hormones.

Benign stromal tumors are thecomas and fibromas, malignant types include granulosa cell tumors, granulosa-theca tumors, and Sertoli-Leydig cell tumors, which are usually considered low-grade cancers.

There also exist **mixed** tumors, containing elements of more than one tumor histology, or so called **secondary cancer**, which results from metastasis from the primary cancer elsewhere in the body, preferential from the breasts or the gastrointestinal tract (Krukenberg cancer).

1.3.2. Staging and Grading

Ovarian cancer **staging** is classified by the FIGO (International Federation of Gynecology and Obstetrics) staging system and is subdivided into four stages:

Stage I: The cancer is limited to one or both ovaries.

Stage II: Pelvic extension or implants can be detected.

Stage III: There are microscopic peritoneal implants outside of the pelvis or limited to the pelvis with extension to the small bowel or omentum.

Stage IV: Distant metastases to the liver or outside the peritoneal cavity occur.

This organization works together with the American Joint Committee on Cancer (AJCC), which classifications are used in all types of cancer. The classification of this organization describes the extent of the primary Tumor (T), the absence or presence of metastasis to nearby lymph Nodes (N), and the absence or presence of distant Metastasis (M) [9].

Tumor **grade** generally refers to the dimension of differentiation of the tumor cells. The higher the grade, the more likely it is that the cancer will spread. According to the American Cancer Society there are three grades:

Grade 1: The cells are well differentiated and look like normal ovarian tissue. They usually grow slowly and are less likely to spread.

Grade 2: The cells are not as well differentiated and look more abnormal.

Grade 3: The cells are poorly differentiated, do not look like ovarian tissue, and are likely to spread. [10]

1.3.3. Risk Factors and Causes for Epithelial Ovarian Cancer

There are many different theories about the causes of ovarian cancer. It is obvious to look at the things that change the risk of ovarian cancer, e.g. age: the risk of developing ovarian cancer gets higher with age. Ovarian cancer is rare in young women, most of the cases occur after menopause, half of all ovarian cancers develop in women over the age of 63. It is thought that there may be some connections between ovulation and the risk of developing ovarian cancer. This theory gets confirmed by the fact, that pregnancy and oral contraceptives both lower the risk of ovarian cancer and both of these things reduce the number of ovulations. [11]

Besides, it is known that tubal ligation and hysterectomy decrease the risk of gaining ovarian cancer. One theory to explain this is that some cancer-causing substances may enter the body through the vagina and pass through the uterus and fallopian tubes to reach the ovaries. This would explain the effect of removing the uterus or blocking the fallopian tubes on ovarian cancer risk. But as mentioned below, there is no stringency that chemicals lead to ovarian cancer. Another theory indicates that androgens can cause ovarian cancer. This is supported by the result of a study that taking the drug danazol may increase ovarian cancer risk (danazol is taken to relieve heavy periods, pain, and infertility caused by endometriosis) [12]. Some recent studies suggest women using estrogen replacement therapy and hormone replacement therapy after menopause have an increased risk of developing ovarian cancer. The risk seems to be higher in women taking estrogen alone (without progesterone) for many years (at least 5 or 10). The increased risk is less certain for women taking both estrogen and progesterone [13].

Certain genes that slow down cell division, cause cells to die at the appropriate time, or help repair DNA damage are called tumor suppressor genes (TSG). Their products are able to suppress tumor formation in their wild type form. Other genes that inter alia promote cell division are called oncogenes. DNA aberrations, like point mutations and deletions, are ways to cancerogenesis. Also hypermethylation that inactivates tumor suppressor genes can cause cancer. Unlike oncogenes, TSG act recessively and therefore, both alleles have to be affected. These mutations mainly occur successively rather than simultaneously, whereas the first silenced allele of a TSG can increase the probability of mutation of the second one by means of LOH (loss of heterozygosity), a common occurrence in cancer, which indicates the absence of a functional TSG.

Inherited genetic factors

Although inherited mutations in **BRCA1** and **BRCA2** were first found in women with breast cancer, they are also responsible for most cases of inherited ovarian cancers. These genes act as tumor suppressors and therefore, if a mutation occurs on one of these genes (inherited or acquired), their cancer-preventing proteins are less effective, and the chance of developing breast or ovarian cancer increases.

The lifetime ovarian cancer risk for women with a **BRCA1** mutation is estimated to be between 35% and 70%. For women with **BRCA2** mutations the risk has been expected to be between 10% and 30% by age 70. These mutations also increase the risks for primary peritoneal carcinoma and fallopian tube carcinoma. In comparison, the ovarian cancer lifetime risk for the women in the general population is about 1.5% [11].

Hereditary nonpolyposis colon cancer (HNPCC, Lynch syndrome): There are 4 different genes involved in this syndrome: *MLH1*, *MSH2*, *MSH6*, and *PMS2*. An abnormal copy of any one of these genes results in a high risk of colon cancer. Women which suffer from this syndrome also have an increased risk of developing endometrial cancer and ovarian cancer. The lifetime risk of ovarian cancer in women with HNPCC is about 10%. This syndrome causes up to 1% of all ovarian epithelial cancers.

People with the rare **Peutz-Jeghers syndrome** develop polyps in the stomach and intestine during adolescence. They have a high risk particularly of cancers of the digestive tract (oesophagus, stomach, small intestine, and colon). Women with this syndrome have an increased risk of ovarian cancer.

Acquired genetic changes

Most DNA mutations that lead to ovarian cancer are not inherited but can be traced back to environmental influence. Acquired mutations of oncogenes and/or tumor suppressor genes in several types of cancer may originate from radiation or cancer-causing chemicals, but there is no evidence for this in ovarian cancer. As yet, studies could not find a notably link between any single chemical in the environment to mutations that cause ovarian cancer.

Most ovarian cancers have several acquired gene mutations. Research lets suggest that tests to identify acquired changes of certain genes, such as the *p53* tumor suppressor gene or the **HER2** oncogene, in ovarian cancers may help predict a woman's prognosis.

1.4. TGF β -Signalling in Normal OSE and Ovarian Carcinomas

Ovarian surface epithelium (OSE) is a monolayer of cuboidal cells supported by a basement membrane and connected by desmosomes and tight junctions. Stationary OSE of a non-ovulating ovary display both epithelial and mesenchymal characteristics but interestingly, OSE express little or no E-cadherin but constitutively express the mesenchymal intermediate filament vimentin [1].

In the course of growth and rupture of ovarian follicles during ovulation cells of the ovarian surface epithelium (OSE) need to proliferate, become quiescent or undergo apoptosis in order to maintain the epithelial covering of the ovary. The periodic wound healing accomplished by OSE is thought to put these cells at risk for transformation and the development of ovarian carcinoma [14]. Transforming growth factor β (TGF β) is one of the growth factors that regulate the tightly controlled proliferation of OSE in response to the reproductive cycle. TGF β isoforms are differently expressed in diverse compartments of the ovary. Human OSE express all three TGF β isoforms, LTBP, TGF β I and TGF β II [15]. TGF β acts as an autocrine growth inhibitor for OSE and in primary epithelial cancer cell cultures obtained from ascites [16]. In contrast epithelial ovarian cancer cell lines are resistant to TGF β mediated growth inhibition [17]. Moreover increased TGF β 1 and LTBP-1 expression as well as TGF β receptor levels were found in more aggressive ovarian carcinomas [18]. These data let suggest that TGF β prevents aberrant proliferation of normal OSE, while the inhibitory actions are overcome in late stage ovarian cancer where TGF β promotes tumor growth and metastasis [19].

1.5. EMT in Ovarian Tumor Progression

Epithelial to mesenchymal transition (EMT) is a highly conserved and fundamental process which governs morphogenesis in multicellular organisms. A phenotypical transition involves the loss of epithelial markers such as components of cell-to-cell contacts (E-cadherin, catenins and cytokeratins), but also needs a de novo expression of mesenchymal markers, including vimentin, fibronectin, and N-cadherin. EMT plays a crucial role during ontogenesis and pathological events like wound healing, but also in late stage tumor progression which leads to invasion and metastasis.

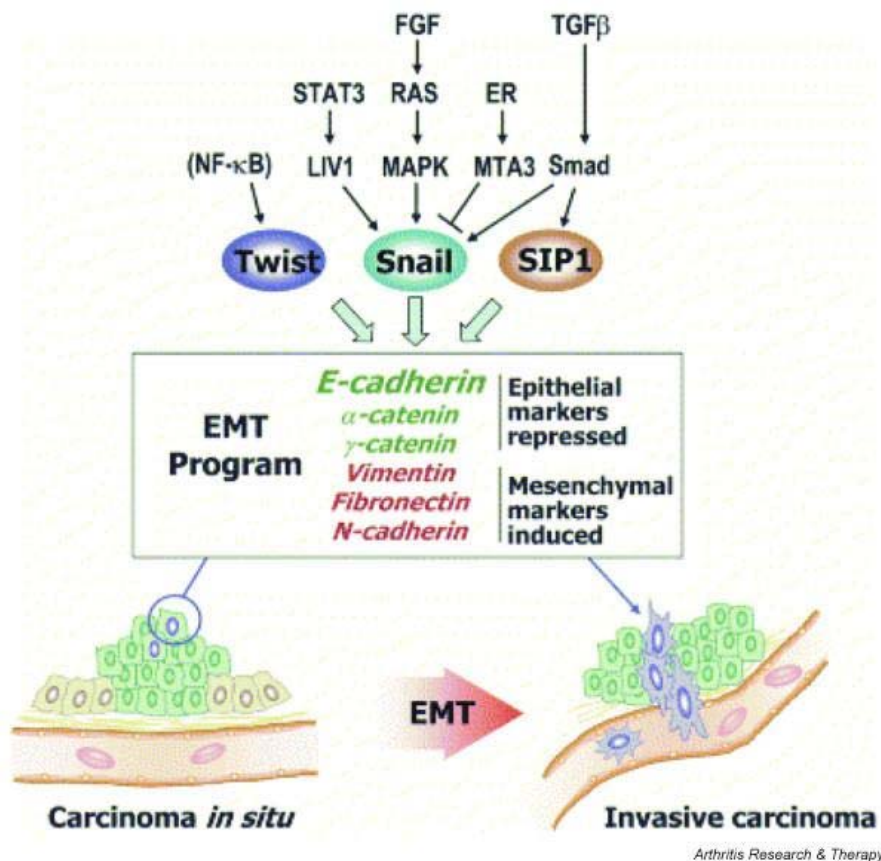


Figure 4 Drivers and mediators of Epithelial-Mesenchymal Transition (EMT) (Zvaifler Arthritis Research & Therapy 2006)

In culture OSE undergo EMT and acquire a fibroblastoid phenotype. They lose epithelial markers such as desmoplakin and keratin and secrete collagen type I and III [20]. Cell culture conditions are thought to mimic the postovulatory situation, where OSE undergo EMT as a wound healing response. Furthermore EMT of normal OSE might also be a physiological event that enables displaced cells which trapped in the postovulatory follicle to acquire a stromal phenotype, preventing the formation of epithelial inclusion cysts. Ovarian carcinomas display a more differentiated epithelial phenotype. E-cadherin expression is most frequently reconstituted in primary ovarian carcinomas enabling tumors to form polarized epithelia, cysts and glandular structures. This differentiated epithelial phenotype is lost in advanced carcinomas in which E-cadherin expression is absent [21]. These data show a dual role of EMT in ovarian tumor progression: EMT of normal OSE is a physiological, possibly tumor suppressive event and MET-like reconstitution of E-cadherin expression is critical for malignant transformation while EMT in late stage carcinogenesis might be the reason for dedifferentiation and increased invasiveness.

1.6. *TUSC3* / *N33*

Studies of human ovarian carcinoma specimens have revealed several types of genetic alterations. Mutation of the *p53* tumor suppressor gene (TSG) is the most frequently identified alteration in serous and poorly differentiated epithelial ovarian carcinoma. Proto-oncogene such as *c-myc*, *K-ras*, *AKT*, and members of the *EGF/ErbB* family of receptor tyrosine kinases, whose products are all involved in the control of growth stimulatory and cell death pathways, were found amplified or mutated in ovarian carcinoma [22].

Loss of heterozygosity (LOH) on chromosomal band 8p22 in ovarian tumors is relatively high, as shown in several studies including a metaanalysis by Pils et al. This observation points towards the possibility that the region harbours potential TSGs [23] [24].

All 22 known genes on this chromosomal band were evaluated using all available public gene profiling data and other published information to select the most probable TSG candidates. On the basis of these previous investigations, eight genes worthy of further examination were identified, one of them called *N33/TUSC3*.

The expression of these eight genes was quantified in a considerable number of primary ovarian carcinoma cell lines (commercially available; EDACC and ATCC) and tumor specimens (58 tumor samples; with Affymetrix GeneChips by Santa Clara, CA) and correlated to clinicopathologic characteristics and survival.

N33 and *EFA6R* showed a significantly decreased expression in tumors of higher grade versus normal ovarian samples or tumors of low grade, potentially reflecting the loss of this gene as a relatively late event in ovarian carcinogenesis. The expression of this gene – together with *EFA6R* - has also an apparent impact on survival.

Because only for *N33* hypermethylation data are available for one tumor entity (colorectal carcinoma), this gene was picked up for further investigations.

Besides, the expression of *N33* was higher in cell lines than in primary tumors. It could have an anti-tumor effect, which is not relevant for proliferation in vitro. In combination with the finding that expression of *N33* is lower only in tumors of advanced grade and FIGO stages, and in patients with relapse, this may indicate that *N33* is involved in later events like metastasis rather than in tumorigenesis [24].

The expression of *N33* was significantly lower in tumors of higher grade (late affected), and its expression often was completely lost in cancer cell lines rather pointing toward a

cell autonomous phenomenon on a genetic or epigenetic basis. Loss of the expression of *N33* and *EFA6R* had a significant impact on overall survival, which was independent from tumor grade and might be a useful prognostic marker in future [24].

TUSC3, originally named *N33*, was identified as a potential TSG from the chromosomal band 8p22 in prostate cancer in the mid 1990's [25, 26]. High homology of *TUSC3* with *OST3*, a subunit of the oligosaccharyltransferase complex impairing N-glycosylation in *Saccharomyces cerevisiae* [27, 28], suggest that *TUSC3* is involved in N-glycosylation of proteins.

Changes in glycosylation of proteins are a long known phenomenon going along with tumor progression. Substantial evidence for this was provided by cancer biologists for dozens of years but functional explications remained somewhat unsatisfactory [29, 30]. In particular, alterations of the relative amount of sialic acids, generally found at the terminus of oligosaccharides on glycoproteins were shown to be associated with cancer cell behavior, such as invasiveness and metastasis [31, 32]. Essentially two mechanisms were considered for this changes, increased enzyme activities of proteins directly involved in sialylation [33] or availability of possible sialylation sites predetermined by the branching of N-glycans [34]. Well known examples for differential sialylations are cytokine receptors such as EGFR, TGF β R, PDGFR, and FGFR and integrin β 1 [35]. In opposition to the apparently relevance of glycosylation for tumor biology the mechanisms of regulation still are mostly unidentified and would require increasing scientific efforts for clarification.

1.7. Glycosylation and Cancer

Sugar chains (glycans) are often attached to proteins and lipids and have multiple roles in the organization and function of all organisms. They participate in activities as diverse as protein folding, leukocyte physiology, and microbial pathogenesis.

Altered glycosylation is a universal feature of cancer cells, and certain types of glycan structures are well-known markers for tumor progression. The changes that occur in malignant cells can take a variety of forms. Examples have been found of loss of expression or excessive expression of certain structures, the persistence of incomplete or

truncated structures, the accumulation of precursors, and, less commonly, the appearance of novel structures. [36]

The classic observation of increased wheat-germ agglutinin binding to animal tumor cells is most likely explained by an overall increase in cell surface sialic acid content, which in turn reduces attachment of metastatic tumor cells to collagen type IV and fibronectin. The epitope Sia α -2-6GalNAc α 1-0 Ser/Thr (called sialyl-Tn) is currently a target for attempts at immunotherapy in some cancers. [36]

What remains to be shown is the precise mechanism(s) by which this biochemical and structural change results in the biological outcomes observed.

2. Methods

2.1. Establishing of cell line models

All cells were cultured in medium (MDAH 2774: RPMI, H134: DMEM, MIA PaCa-2: α -MEM, SKOV3: McCoy's) with 10% FCS (fetal calf serum), 50 units ml^{-1} penicillin G, and 50 $\mu\text{g ml}^{-1}$ streptomycin sulphate at 37°C in a humidified atmosphere of 95% air and 5% CO_2 .

Human ovarian carcinoma cell lines MDAH 2774 Co and MDAH 2774 BAMBI (*TUSC3* silenced) were originally morphologically different single-cell clones from MDAH 2774, an ovary adenocarcinoma cell line, received from the ATCC (CRL-10303). In this cell line, *TUSC3* was silenced with the vector Ambion's pSilencerTM 4.1-CMV neo, designed for long term gene silencing experiments which carries a RNA polymerase II-type CMV promoter (human cytomegalovirus immediate-early promoter) and an optimized SV40 polyadenylation signal to drive high level expression of hairpin siRNA. The SV40 promoter expresses an antibiotic resistance gene for neomycin (G418) suitable for long-term antibiotic selection.

For the reconstitution of *TUSC3* expression the IMAGE clone (BC010370 in pDNR-LIB) was cloned in the expression vector pLP-IRESneo and for the *TUSC3*-FLAG-fusion protein the FLAG-peptide was cloned in frame to the C-terminus of *TUSC3*. As control the empty vector pLP-IRESneo was employed. (H134, MIA PaCa-2)

Transfections were performed with lipofectamine 2000 (Invitrogen, Carlsbad, CA, USA) and stable clones were selected with G418 (MDAH 2774 and H134: 700 $\mu\text{g ml}^{-1}$, MIA PaCa-2: 800 $\mu\text{g ml}^{-1}$) and subcultured with half concentrations of G418. Growth with TGF- β was performed in growth medium supplemented with 1 or 2.5 ng ml^{-1} TGF- β for at least one week with medium change every second day.

Plasmid growth in liquid medium (AP: 50 mg/ml; CM: 25 mg/ml)

Plasmid extraction („KochQuickly“)

harvesting *E. coli*

+350 μl STET buffer

STET Buffer:

10 mM Tris-Cl pH 8,0

0,1 M NaCl

1 mM EDTA pH 8,0

5 % (v/v) Triton X-100
+ 10 µl lysozyme
5 min incubation
40 sec 99°C, on ice immediately
15 min centrifugation at 4°C
remove pellet
+ 350 µl isopropanol, vortex
15 min centrifugation at 4°C
discard supernatant, dry pellet, resuspend pellet in 30 µl T1/10E

Plasmid Maxi-Prep (Qiagen Plasmid Purification Kit, Qiagen GmbH)

Digestion

2 µl DNA
2 µl buffer
0,2 µl BSA
0,2 µl RNase
1 µl enzyme
14,6 H₂O

PCR purification (QIAquick PCR Purification Kit, Qiagen GmbH)

eluate with 40 µl dH₂O

“Fill in” - reaction (sticky ends)

40 µl DNA
2 µl DNA-polymerase 1
1 µl dNTP 1 mM
0,5 µl BSA
5 µl NEB2
1,5 µl H₂O
20 min at 37°C

Gel-extraction (illustra GFX PCR DNA and Gel Band Purification Kit, GE Healthcare)

eluate with 2 x 50 µl TE

DNA precipitation

+ 10% NaAcetate
+ 2,5 x EtOH 100% -20°C
30 min centrifugation at 4°C
wash with 70% EtOH
resuspend pellet in 7 µl dH₂O

Ligation

1 µl 10 x buffer
0,9 µl T4 DNA ligase
5 µl insert
3,1 µl vector
60 min 24°C
48 h 16°C

Transformation into DH5 α

sample of ligation + 50 μ l competent cells
incubate 20 min on ice
40 sec 42°C
1 min on ice
+ 250 μ l LB medium, vortex
50 min at 37°C
-> plating (AP: 100 mg/ml; CM: 30 mg/ml)

Transfection

5 μ g plasmid DNA
12 μ l lipofectamine 2000
138 μ l OptiMEM
20 min incubation in 2 ml OptiMEM
after 4-5 h medium (depending on whether RPMI, DMEM, α -MEM, or McCoy's)

2.2. RNA-Isolation

The cells were grown in a middle flask and their RNA was purified using the RNeasy Mini Kit (spin protocol) from Qiagen GmbH (Qiagen, Hilden, Germany). After the cells were harvested at 1200 rpm for 6 minutes, they were washed once and disrupted by addition of 350 μ l Buffer RLT. Then the sample was homogenized using a QIAshredder spin column, precipitated with 350 μ l 70% ethanol and applied to an RNeasy mini column, which was washed two times with buffers RW1 (700 μ l) and RPE (500 μ l) and finally eluted with 40 μ l RNase-free water. The RNA yield of the eluate was determined using a UV-spectrometer or a NanoDrop spectrometer ND-1000 (peqlab Biotechnologie GmbH, Linz, Austria).

2.3. cDNA Synthesis

Up to 1 μ g RNA was treated with the First Strand cDNA Synthesis Kit (Fermentas, St. Leon-Rot, Germany) adding dNTPs, anchored oligo-(dT) and random nonamer primers (Sigma-Aldrich, Saint Louis, MO, USA) in a PCR-tube, which was incubated 10 minutes at 70°C. After cooling down on 4°C 5 x buffer, RNase inhibitor and avian reverse transcriptase by Fermentas were added. One cycle of a PCR was performed for 10 minutes at 25°C, 40 minutes at 46°C, and 20 minutes at 65°C, followed by cooling down at 4°C until the sample was used for real time PCR.

1,5 µl dNTP
1,0 µl 1:1 mix random nonamers + oligo-(dT)
8,5 µl RNA
(10 min 70°C)
3,0 µl 5 x buffer
0,5 µl reverse transcriptase
0,5 µl RNase inhibitor

2.4. Quantitative Real Time RT-PCR

2µl cDNA of each template were mixed in duplicates with 10µl 2 x qPCR Mastermix Plus (Eurogentec Deutschland GmbH, Köln, Germany) with 7.5µl PCR-water using the following Assay-on-Demand™ probes: Hs00185147_m1 for *TUSC3* and Hs99999909_m1 for *HPRT1* as house-keeping control (Applied Biosystems, Foster City, CA, USA). Expression is given in arbitrary units and was calculated with GeneAmp5700 SDS Software as described in Pils et al., 2005 [24].

2.5. Protein extraction

Cells were cultured in 10 cm cell culture dishes up to 100% confluence and were washed two times with cold PBS. Then they were lysated with RIPA⁺-buffer (containing 1/100 Na-orthovanadate and 1/25 25 x Complete by Roche Ltd, Basel, Switzerland), incubated on ice for 5 minutes and carefully scraped with a cell scraper. The lysate was vortexed several times and centrifuged 30 minutes at full speed. The supernatant was saved and stored at -80°C.

A Bradford-Assay (Sigma-Aldrich, Saint Louis, MO, USA) was used to determine the concentration of proteins: In a 96-well ELISA plate 200µl Bradford reagent was mixed with 2µl of the sample in duplicates, and with 5µl of the standard dilutions with defined concentrations for standardization, respectively. The absorption was measured with a Wallac 1420 Victor².

2.6. Western Blot

Electrophoresis

30ng protein was mixed with 50% 2 x loading buffer (incl. 3% β-mercaptoethanol), heated up for 5 minutes to 70°C, loaded onto a 12% polyacrylamid gel and separated by the usage

of gel electrophoresis. As a marker, a Precision Plus Protein Dual Color Standard (Bio-Rad, Hercules, CA, USA) was loaded onto the gel too.

12% polyacrylamid gel (20 ml)

6,6 ml H₂O
8,0 ml 30% acrylamide mix
5,0 ml 1,5 M Tris pH 8,8
0,2 ml 10% SDS
0,2 ml 10% ammonium persulfate
0,008 ml TEMED

5% stacking gel (4 ml)

2,7 ml H₂O
0,67 ml 30% acrylamide mix
0,5 ml 1,0 M Tris pH 6,8
0,04 ml 10% SDS
0,04 ml 10% ammonium persulfate
0,004 ml TEMED

Electro blotting

A polyvinylidenfluorid (PVDF) membrane Amersham Hybond-P (GE Healthcare, Vienna, Austria) was wetted with methanol and water and then equilibrated in transfer buffer. The gel and the membrane were given into an electro blotting cassette (Bio-Rad, Hercules, CA, USA), which was placed in a transfer buffer between two electrodes. The transfer time was 90 minutes at 350 amperes. After the transfer, the membrane was dried with methanol to fix the proteins on it and then was blocked with 10% Western Blocking Reagent (Roche, Basel, Switzerland) in PBS-Tween (incl. 0.01% Tween) for one hour (or over night).

Incubation with antibodies

Thereafter, the membrane was incubated particular with the first (one hour or over night) and the second (45 minutes) antibodies on a rotary shaker, each antibody diluted in PBS-Tween with 5% blocking reagent. The optimal dilution was determined empirically for each antibody, between the first and the second antibody the membrane was washed 2 times for 5 minutes, after the second antibody 4 times for 5 minutes.

Detection

For antibody detection ECL Western Blotting Detection Reagents by GE Healthcare was prepared and the membrane was incubated one minute. After this, the membrane was exposed to an autoradiography film.

Stripping

To apply some more antibodies on the same membrane, it had to be stripped (to detach the previous antibodies). Therefore, a stripping buffer is mixed with SDS, TrisHCl and β -mercaptoethanol, in which the membrane is incubated at 55°C and then washed with fluency water for one hour. Then the membrane has to be dried, blocked and incubated with the antibodies as desired in the way described above.

The antibodies used were: anti-nucleoporin p62 (BD Biosciences, San Jose, CA, USA), 1:1000; mouse anti-FLAG M2 antibody (10 $\mu\text{g ml}^{-1}$, Sigma Aldrich, Saint Louis, MO, USA), 1:1000; mouse anti-FLAG (F2555, Sigma Aldrich), 1:1000; goat anti-integrin $\beta 1$ (R&D, Minniapolis, MN, USA), 1:1000; rabbit anti-calnexin (personal gift of E. Ivessa) 1:1000; goat anti-mouse HRP-conjugate (Calbiochem, Darmstadt, Germany), 1:10000; rabbit anti-actin HRP-conjugate (Santa Cruz Biotechnology, Santa Cruz, CA, USA), 1:500; donkey anti-goat-HRP-linked (Santa Cruz Biotechnology, Santa Cruz, CA, USA), 1:10000.

Buffer composition

1 x PBS pH 7,4 (1 liter)

137 mM NaCl (8g)

2,7 mM KCl (0,2g)

10 mM Na_2HPO_4 (1,44g)

2 mM KH_2PO_4 (0,24g)

2 x SDS Gel-loading Buffer

100 mM Tris-Cl pH 6,8

4% (w/v) SDS (electrophoresis grade)

0,2% (w/v) bromophenol blue

20% (v/v) glycerol

200 mM dithiothreitol or β -mercaptoethanol (fresh added bevore use)

5 x Running Buffer pH 8,3 (1 liter)

25 mM Tris (15,1g)

250 mM Glycine (94g)

0,1 % SDS (50 ml of a 10% stock)

1 x Blotting Buffer (1 liter)
25 mM Tris-Cl (100 ml of a 10 x stock)
250 mM Glycine
0,1% SDS (1 ml of a 20% stock)
20% MetOH

Stripping Buffer (100 ml)
800 µl β-mercaptoethanol
20 ml 10% SDS
12,5 ml 0,5 M Tris-HCl pH 6,8
67,5 ml H₂O

Sub-cellular fractionation

(Cooperation with Wolfgang Gregor, Research Group of Molecular Pharmacology and Toxicology, University of Veterinary Medicine Vienna, Austria)

For localization experiments subcellular fractions (microsomes, soluble cytoplasm, mitochondria, lysosomes, and nuclei) were prepared according to a consecutive centrifugation protocol:

Cells grown in T75 flasks were harvested in appropriate medium with a rubber policeman and collected at 270 g for 10 minutes. The cells were resuspended in medium and treated with 20ng ml⁻¹ TGF-β for 9 minutes at room temperature. Then the cells were immediately harvested at 4300 g and 4°C for 4 minutes, resuspended in 3 ml buffer A (250mM sucrose, 10mM triethanolamine, pH 7.4, 1mM EGTA) complemented with Complete protease inhibitors (Roche Ltd, Basel, Switzerland) and phosphatase inhibitor cocktail II (Sigma-Aldrich, St. Louis, MO, USA) and lysed with a tightly fitting Potter Teflon pestle for 4 minutes. Nuclei and unbroken cells were pelleted at 1000 g for 10 minutes and resuspended in 4 ml 2.2 M sucrose, 1mM MgCl₂, 10mM Tris, pH 7.4 with a loose Potter pestle. Pure nuclei were repelleted at 70,000 g for 80 min in a Beckman L8-M ultracentrifuge (SW 50.1 rotor) and washed with 4 ml buffer A at 1000 g. The mitochondria and lysosomes were pelleted from the post-nuclear supernatant at 20,200 g for 15 minutes. The microsomes were pelleted from the last supernatant at 182,000 g for 40 minutes and washed with 4 ml buffer A. The post-microsomal supernatant was kept as the cytosolic fraction. The final pellets were resuspended in buffer A and stored at -20°C. All centrifugation and resuspension steps were performed at 4°C. For Western analysis, 5

µg protein of each subcellular fraction (except 15 µg for the cytoplasmic fraction) was lysed, attenuated, and loaded.

Lysis Buffer

0,6 ml H₂O

0,4 ml NaEDTA 0,5 M, pH 8,0

1 ml 20% SDS

The purity of these fractions was analyzed with antibodies against marker proteins (nucleoprin p62, cox 5a, ribophorin I, and β-actin for above fractions, respectively).

The antibodies used were: anti-nucleoporin p62 (BD Biosciences, San Jose, CA, USA) 1:1000; rabbit anti-ribophorin I (personal gift of E. Ivessa) 1:1000; mouse anti-cox 5a (Molecular Probes, eubio, Vienna, Austria), 1:1000; rabbit anti-actin HRP-conjugate (Santa Cruz Biotechnology, Santa Cruz, CA, USA), 1:500; goat anti-mouse HRP-conjugate (Santa Cruz Biotechnology, Santa Cruz, CA, USA) 1:6000.

2.7. Proliferation

Proliferation (doubling time) was measured in triplicates by subsequent cultivation in 6-well plates and cell counting by CASY cell counter (Innovatis AG, Bielefeld, Germany). Therefore, cells were trypsinized, took up in 1 ml medium, and 20 µl were diluted in 10 ml CASYton. Doubling time (t_d) was calculated as follows: $\mu = (\ln(x_t) - \ln(x_0)) / t$, $t_d = \ln(2) / \mu$ (x_t , cell number at time t ; x_0 , cell number at start of experiment; t , duration of experiment).

2.8. Apoptosis Assay

Apoptosis was detected by FACS analysis with Annexin V-FITC (Beckman Coulter, BD Biosciences, San Jose, CA USA) and with ApoONE Homogeneous Caspase-3/7 Assay (Promega, Madison, WI, USA). The cells were grown in triplicates for one week with 5ng ml⁻¹ TGFβ in a 6-well plate (4x10⁵) for Annexin V-FITC assay and in a 96-well plate (2x10⁴) for ApoONE assay, respectively. For a positive control, some cells were stimulated with 100ng ml⁻¹ TRAIL 24 hours before testing, for a negative control, some cells remained untreated.

The ApoONE reagent was incubated for 2-4 h and the absorption was measured with a Wallac 1420 Victor². For FACS analysis, cells were treated with Annexin V-FITC and

Propidiumiodid (PI), according to the manufacturer's instruction and fluorescence was measured with a BD FACScanTM Flow Cytometer (BD Biosciences, San Jose, CA USA).

2.9. Adhesion Assay

For the adhesion assay, 96-well ELISA plates were coated with collagen I ($3\mu\text{g}/0,3\text{cm}^2$), collagen IV ($3\mu\text{g}/0,3\text{cm}^2$), laminin ($0,6\mu\text{g}/0,3\text{cm}^2$), fibronectin ($0,75\mu\text{g}/0,3\text{cm}^2$), and 0,2% BSA, for 2 hours. Then, 3×10^4 cells were seeded for 30 minutes, washed, and remaining cells were quantified with the Cell Titer-Blue[®] cell viability assay (Promega, Madison, WI, USA).

For the adhesion assay with hyaluronic acid, the ELISA plate was coated for 16 hours in different concentrations (1mg/ml, 0,1mg/ml, 0,01mg/ml) and with 0,2% BSA. After that, 3×10^4 cells were seeded (in triplicates), the plate was centrifuged with 650 rpm for 2 minutes and incubated for further 5 minutes, washed, and remaining cells were quantified with the Cell Titer-Blue[®] cell viability assay.

2.10. Migration and Invasion Assays

Migration and invasion assays were performed in a 24-well plate trans-well system (BD Biosciences, San Jose, CA, USA). For migration and invasion assays, $2,5 \times 10^4$ cells were seeded in triplicates on the $8.0 \mu\text{m}$ pore size control chambers for migration and the BD Matrigel invasion chambers (pore size: $8.0 \mu\text{m}$) for invasion. 30% FCS was used as chemo-attractant. After 24 h incubation cells from both sides of the membrane were trypsinized, harvested and reseeded in 96-well plates in appropriate densities. After 16 h of growth, cell numbers were estimated by the Cell Titer-Blue[®] cell viability assay, based on conversion of resazurin to fluorescent resorufin (Promega, Madison, WI, USA). Results were given in percent calculated as follows: after subtraction of blank values, the fluorescence ($560_{\text{Ex}}/595_{\text{Em}}$ nm) in cells from the lower side of the membrane (corresponding to the migrated/invaded cells) was divided by the sum of fluorescence values in cells from both sides of the filter (corresponding to all seeded cells) and multiplied with 100.

Chick chorioallantoic membrane (CAM) Invasion Assay (cooperation with Daniel Hollwedel and Barbara Kapeller, IBF-Institute for Biomedical Research, Medical University of Vienna, Austria)

Besides, the invasiveness was tested in chicken eggs, an animal substitute model: The chick chorioallantoic membrane (CAM) assay is a well established model for examine toxicity and irritation studies, but also for tissue engineering tasks, transplantation and angiogenesis. Chicken eggs in the early phase of breeding are between in vitro and in vivo systems but may provide an immunodeficient, vascularized test environment [39].



Figure 5 Chorioallantoic Membrane of fertilized Chicken Egg (MB Research Labs)

The cell lines were inoculated on the chorioallantoic membrane of fertilized chicken eggs on day 5 or 6 of breeding. Therefore, a window with about three centimeters of diameter was opened sterile in the flat pole of the eggshell. The cells – about 2×10^6 cells/CAM, grown and suspended in medium without G418 - were applied onto a small patch of the CAM. The egg was incubated in an upright position, covered with tinfoil. At day 10, the embryo was fixed in 10% formaldehyde and the CAM was embedded in paraffin. After hematoxylin/eosin staining, or rather immunohistochemistry with e-cadherin or mesothelin, cell morphology was evaluated.

2.11. Immunocytochemical and immunohistochemical staining

For immunocytochemical staining cells were grown overnight on sterile four-well Lab-Tek™ Chamber Slides™ (Nagle Nunc International, Rochester, NY, USA). After washing with PBS, cells were fixed in 3% formaldehyde/PBS for 20 minutes at room temperature and permeabilized with 0.5% Triton X-100/PBS for five minutes. Endogenous peroxidase activity was blocked by ten minute incubation with 3% H_2O_2 /PBS. Subsequently, cells

were blocked for 30 minutes with 0.2% fish gelatine/PBS and incubated with the primary antibody diluted in 0.2% fish gelatine/PBS for 60 minutes at room temperature.

Dilutions in 0.2% fish gelatine/PBS of primary antibodies were as follows: polyclonal goat anti-integrin $\beta 1$ antibody (R&D, Minniapolis, MN, USA) 1:500, biotinylated sialic acid-specific lectin SNA (Vector Laboratories, Burlingame, CA, USA) 1:200.

After washing with PBS, the secondary antibody, diluted in 0.2% fish-gelatine/PBS was applied for 30 minutes: biotin-conjugated goat-anti mouse (BA9200) 1:200, biotinylated rabbit anti-goat antibody (Vector Laboratories, Burlingame, CA, USA) 1:200. Then the sample was incubated with the streptavidin ABCComplex-HRP (ABC-Kit from Dako, Glostrup, Denmark) for 45 minutes and was stained with DAB+ (Dako) according to the manufacturer's instruction. Finally cells were stained with hematoxyline/eosin and mounted in Eukitt (O. Kindler GmbH, Freiburg, Germany). Microscopy was performed on an Olympus BX50 upright light microscope (Olympus Europe, Hamburg, Germany) equipped with the Soft Imaging system CC12.

For immunohistochemical staining, 5 μ m paraffin sections of the paraffin-embedded tissues were deparaffinized with xylenes and re-hydrated by incubation in serial dilutions of ethanol. Subsequently, antigen retrieval was performed based on a citrate buffer protocol (incubation in 1:20 diluted citrate buffer (pH 9) DEPP-9 (Eubio, Vienna, Austria) at 96°C for 20 minutes). Sections were treated with 3% H₂O₂/PBS (pH 7.4) to quench endogenous peroxidases and blocked with 10% normal goat serum for 30 min. Afterwards the sections were incubated with the first antibody in 10% serum at RT for 60 minutes. After washing with PBS, the second antibody was applied at a 1:200 dilution in 10% serum/PBS for 30 minutes, followed by washing and incubation with the streptavidin ABCComplex-HRP (ABC-Kit, Dako) for 45 minutes. Finally DAB+ (Dako) staining was performed for 10 minutes according to the manufacturer's instruction. Meyer's hematoxyline was used for counterstaining the nuclei. Microscopy was performed on an Olympus BX50 upright light microscope (Olympus Europe, Hamburg, Germany) equipped with the Soft Imaging system CC12.

2.12. Statistical analysis

Continuous variables are presented as mean with standard deviation, categorical variables as absolute and relative frequencies. The significance of differences in doubling time,

migration and invasion was calculated using t-test analysis. In order to compare frequencies between two or more groups, Pearson's Chi-Square test was performed. In case of a sufficient approximation to a normal distribution, mean values and 95% confidence intervals for *TUSC3* expression were calculated on a logarithmic scale and then transformed back to the original scale. In order to compare *TUSC3* expression between two or more groups, a t-test or one-way ANOVA, respectively, was performed using the log-transformed expression as independent variable. The potential influence of *TUSC3* methylation and of FIGO stage on progression free and overall survival is presented in plots of the corresponding Kaplan-Meier estimates. As time point for progression the date of the documentation of the first relapse or the first documentation of the disease progression starting at the time of the first diagnosis was used. Statistical significance for experiments comparing characteristics of the cell line models was calculated with the T-test. P-values ≤ 0.05 were considered to be statistically significant. All computations have been performed using SPSS software version 15.0 (SPSS Inc. Headquarters, Chicago, Illinois, USA).

3. Results

3.1. Present Results:

Following unpublished data by Krainer, Pils et al. are available in our laboratory: By using a systematic expression screening approach on genes of 8p22, we found *N33/TUSC3* to be significantly down-regulated in ovarian cancer tissues. The sample consisted of whole genome gene profiling data (Human Genome Survey Microarray, Applied Biosystems) of 38 epithelial tumor cell lines, 7 of them with absent (4 complete missing and 3 very low) and 31 with 'normal' *TUSC3* expression.

mRNA expression of *TUSC3* was measured by qRT-PCR. It was significantly lower in tumors (0.105 ru) compared to controls (0.465 ru, $P<0.001$).

Using MSP (methylation specific PCR) we found the promoter of *TUSC3* methylated in eleven cell lines which resulted in an undetectable expression of *TUSC3* (or an expression at the lower limit of detection).

30 out of 102 (29.8%) ovarian cancer tissues derived from patients at primary diagnosis showed methylated bands but none of the 20 benign ovarian controls ($P=0.003$). The mean *TUSC3* expression in the methylated group was significantly lower (0.065 ru) compared to the unmethylated group (0.135 ru, $P=0.001$), confirming a similar interrelation of *TUSC3* methylation status and *TUSC3* expression as found in cancer cell lines.

Patients with methylated *TUSC3* had significant shorter progression free (RR 1.97, $P=0.023$) and overall survival rates (RR 2.92, $P=0.007$) as shown in Kaplan Meier estimates (Fig. 6). The median progression free survival was 11.1 months in the methylated group compared to 24.6 months in the unmethylated group.

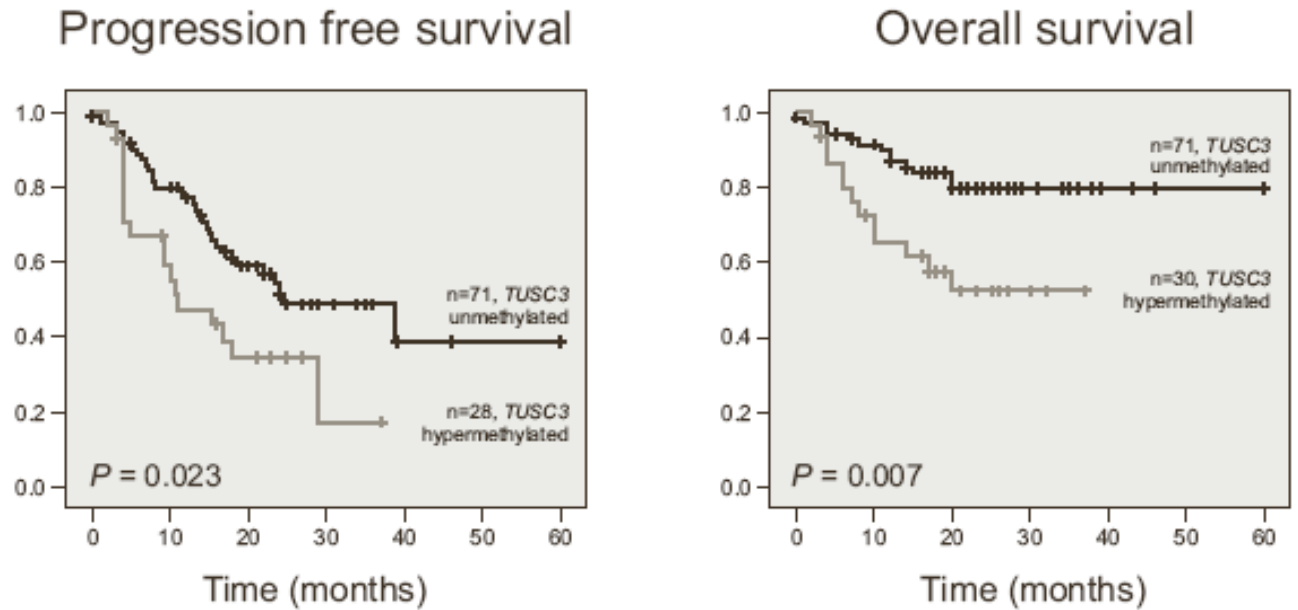


Figure 6 Plots of Kaplan-Meier estimates for progression free and overall survival of patients with tumor samples with hypermethylated or unmethylated *TUSC3*. As time point for progression, the date of the documentation of the first relapse or the first documentation of the disease progression, starting at the time of the first diagnosis was used. P-values are from the univariate Cox regression analysis (Table 1).

Moreover, multiple Cox proportional hazards analyses revealed a significant association between *TUSC3* methylation and progression free (RR 2.17, $P=0.024$) and overall survival (RR 4.12, $P=0.008$) independent from other risk factors, including response to chemotherapy. Hazard ratios for progression free survival were comparable to FIGO stage (RR 2.82, $P<0.001$) and residual disease after surgery (RR 3.04, $P=0.001$), the only other significant prognostic factors available at the time when options for therapy have to be explored.

Table 1 Univariate and Multiple Cox Proportional Hazards Analysis

	Progression free survival			
	Univariate Relative risk (95% CI) [‡]	<i>P</i>	Multiple Relative risk (95% CI) [‡]	<i>P</i>
Age at diagnosis	1.02 (0.99-1.05)	0.184	used	
Histology (non-serous <i>v</i> serous) [†]	1.16 (0.58-2.32)	0.683		
FIGO stage	2.82 (1.87-4.26)	<0.001		
Grading	0.98 (0.58-1.65)	0.933		
Residual disease (>1cm <i>v</i> ≤1cm) [†]	3.04 (1.53-6.02)	0.001		
Therapy response (no <i>v</i> yes) [†]	4.91 (2.64-9.10)	<0.001	used	
Methylation of <i>TUSC3</i> (yes <i>v</i> no) [†]	1.97 (1.10-3.53)	0.023	2.17 (1.11-4.24)	0.024

Overall survival				
	Univariate		Multiple	
	Relative risk (95% CI) [‡]	P	Relative risk (95% CI) [‡]	P
Age at diagnosis	1.06 (1.02-1.10)	0.003	used	
Histology (non-serous v serous) [†]	2.37 (1.05-5.32)	0.037	used	
FIGO stage	2.52 (1.41-4.49)	0.002	used	
Grading	0.76 (0.38-1.53)	0.446		
Residual disease (>1cm v ≤1cm) [†]	5.28 (2.19-12.70)	<0.001	used	
Therapy response (no v yes) [†]	9.56 (3.56-25.65)	<0.001	used	
Methylation of <i>TUSC3</i> (yes v no) [†]	2.92 (1.35-6.29)	0.007	4.12 (1.45-11.65)	0.008

[‡]CI, confidence interval. [†]Categorical variable. Bold, statistically significant.

Moreover the data point to a possible involvement of *TUSC3* on transforming growth factor β (TGF β)-family signalling since *TUSC3* expression is significantly negative correlated to the expression of bone morphogenic protein (BMP) and Activin Membrane Bound Inhibitor (BAMBI) (Fig. 7). Together these data suggest a possible role of *TUSC3* in epithelial to mesenchymal transition (EMT), which is known to be an important event in carcinogenesis.

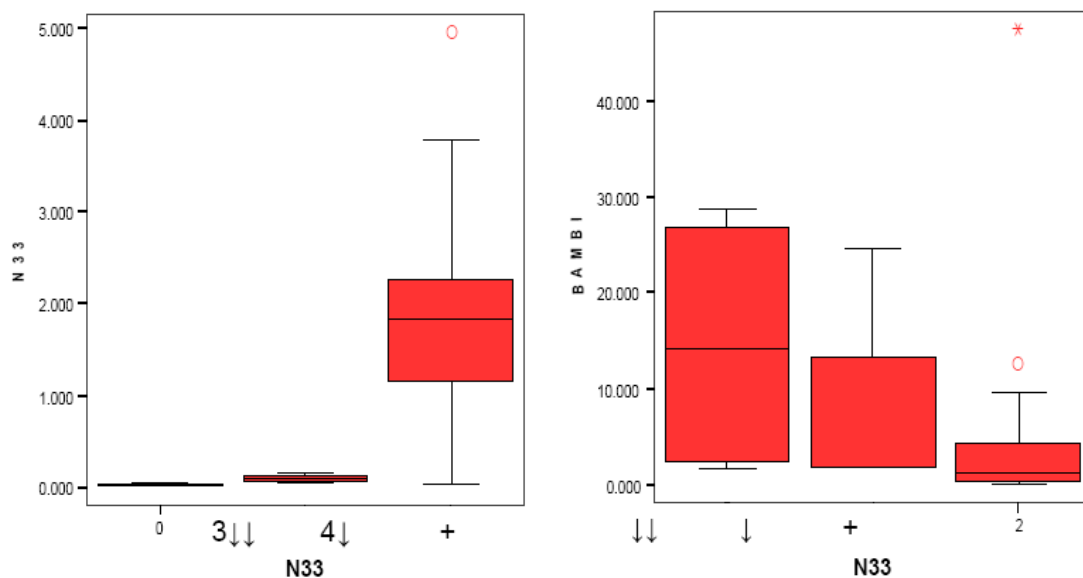


Figure 7 Negative correlation of *TUSC3* (N33) and *BAMBI* expression in 38 cancer cell lines, (0) four cell lines with missing, (1) three cell lines with low, and (2) 31 cell lines with high *TUSC3* expression. Pearson correlation: -0.348, P = 0.033.

3.2. Establishing of cell line models and *TUSC3* expression

To identify the function of *TUSC3*, we employed three independent *in vitro* cancer cell line models based on MDAH 2774, H134, and Mia PaCa-2, the former with an epigenetically silenced *TUSC3* (si*TUSC3*), and the latter two with reconstituted *TUSC3* (TFlag, a FLAG-tagged *TUSC3*, and *TUSC3*).

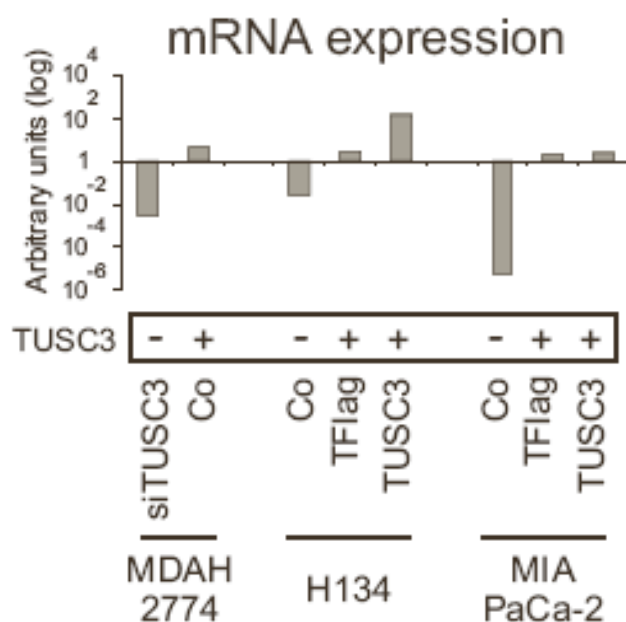


Figure 8 *In vitro* characterization of cell line models with either genetically silenced (MDAH 2774) or reconstituted *TUSC3* expression (H134 and MIA PaCa-2). mRNA expression is shown in arbitrary units.

3.3. Morphology

The cell morphology changed in all three cell line models upon (re)expression of *TUSC3* – most obviously in the MDAH 2774 cells – from a more epitheloid to a more mesenchymal shape, indicated by a disorganized actin stress-fiber network (Fig. 9).

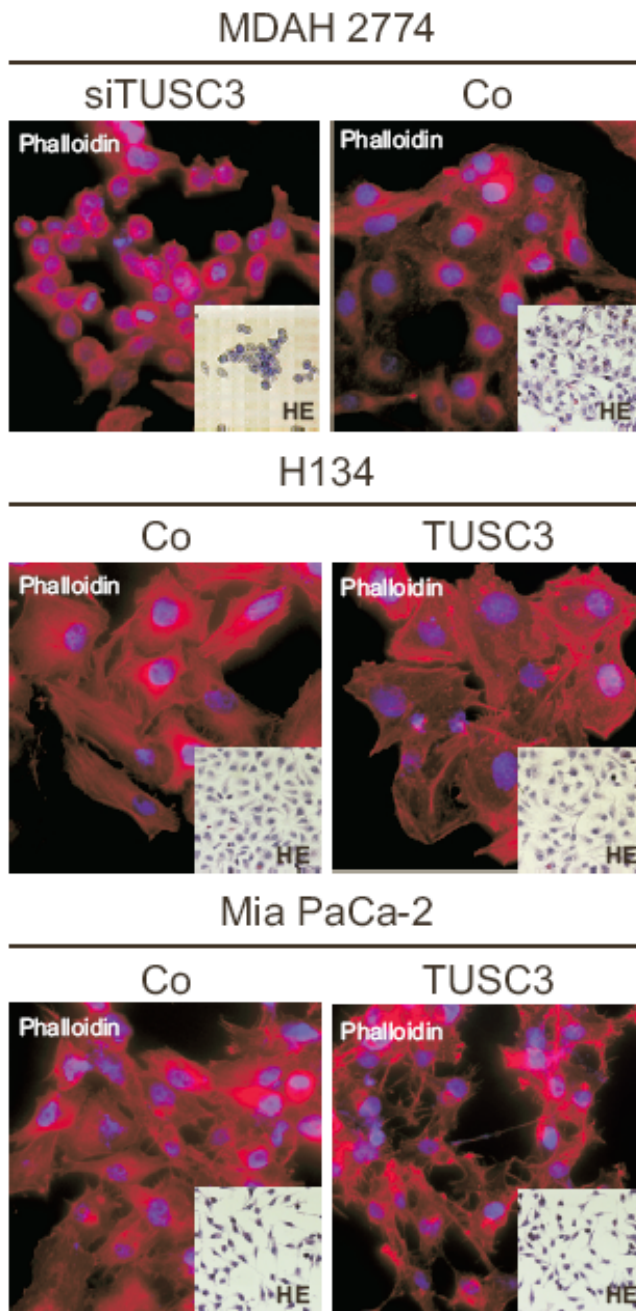


Figure 9 Morphological overview stains with phalloidin (F-actin) and DAPI (nuclei) (large picture) and HE stains (inset) are shown for all three cell lines.

3.4. Proliferation

Proliferation of *TUSC3*-positive cells was always significantly decreased (from 23% to 33%) compared to the *TUSC3*-negative control cells (Fig. 10).

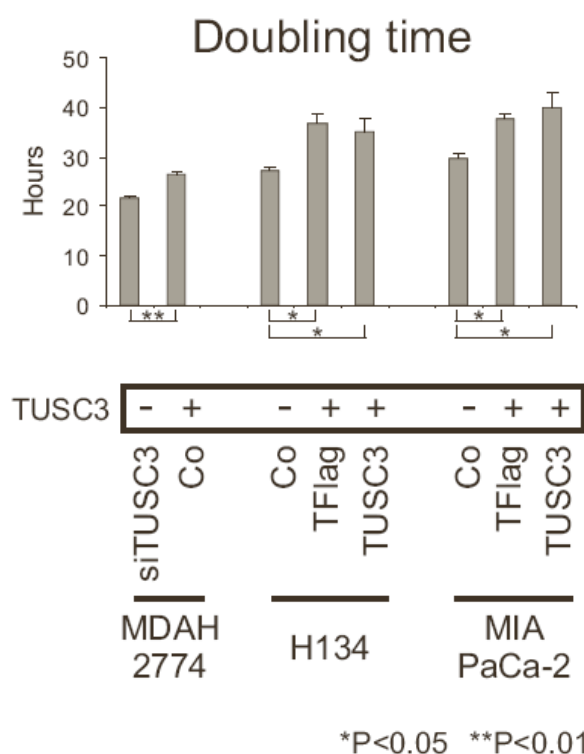


Figure 10 *In vitro* characterization of cell line models with either genetically silenced (MDAH 2774) or reconstituted *TUSC3* expression (H134 and MIA PaCa-2). Doubling time in hours of MDAH2774, H134, and MIA PaCa-2. Experiments were performed in triplicates, the significance was calculated by the T-test and marked by one (P<0.05) or two asterisks (P<0.01).

Analysis of phenotypical characteristics showed significantly increased proliferation rates of MDAH Co compared to MDAH siTUSC3 (+32.1%, P=0.011) and significantly decreased sensitivity to growth inhibition in the presence of 2.5 ng ml⁻¹ TGF-β. Upon TGF-β supplementation proliferation of MDAH Co decreased only by 0.28% (not significant) whereas in MDAH siTUSC3 proliferation decreased significantly (26.7%, P=0.005) (Fig. 11).

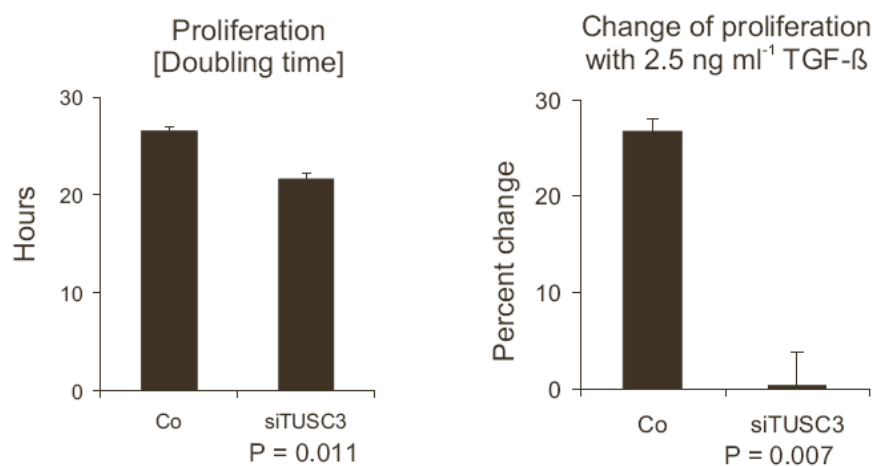


Figure 11 Doubling time of MDAH 2774 with and without TGF- β treatment in hours (left diagram), change of proliferation in percent change (right diagram). TUSC3-positive cells react to TGF- β treatment.

3.5. Apoptosis

Consistent with the decreased TGF- β sensitivity in MDAH siTUSC3, also the rate of apoptosis in the presence of TGF- β was significantly decreased (MDAH Co: 9.8% and 19.0% apoptosis in the absence and presence of TGF- β , respectively, corresponding to an increase of +93.9%; MDAH siTUSC3: 4.5% and 5.1%, +13.3%) (Fig.12).

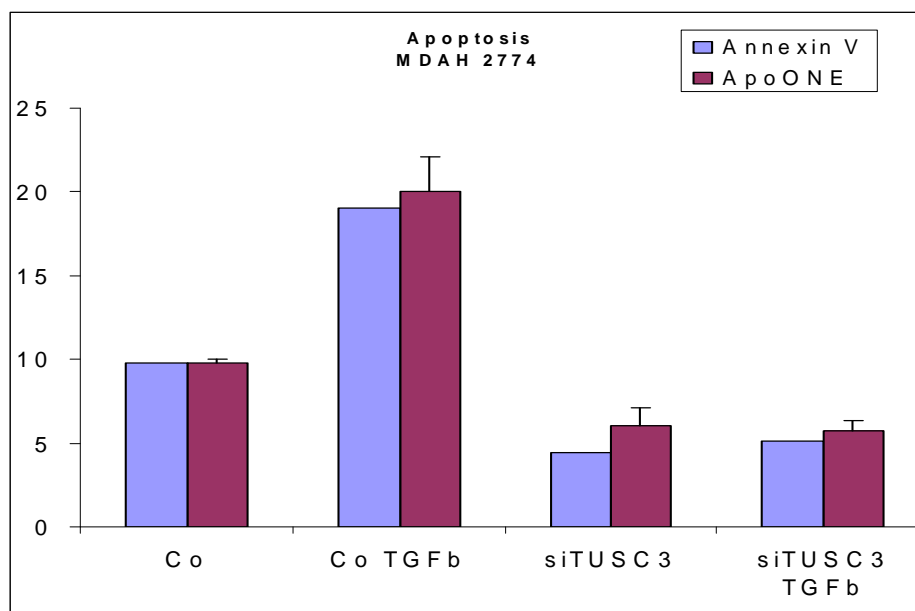


Figure 12 Apoptosis assay (ApoONE and Annexin V-FITC), MDAH 2774; TUSC3-positive cells react to TGF- β treatment.

3.6. Migration and Invasion Assays

The migration ability was significantly increased by higher *TUSC3* expression in both ovarian cancer cell lines (MDAH 2774, H134), but interestingly it was decreased in the MIA PaCa-2 cell line model (Fig. 13). Invasiveness, as tested by a matrigel-transwell assay, never was affected significantly (Fig. 13).

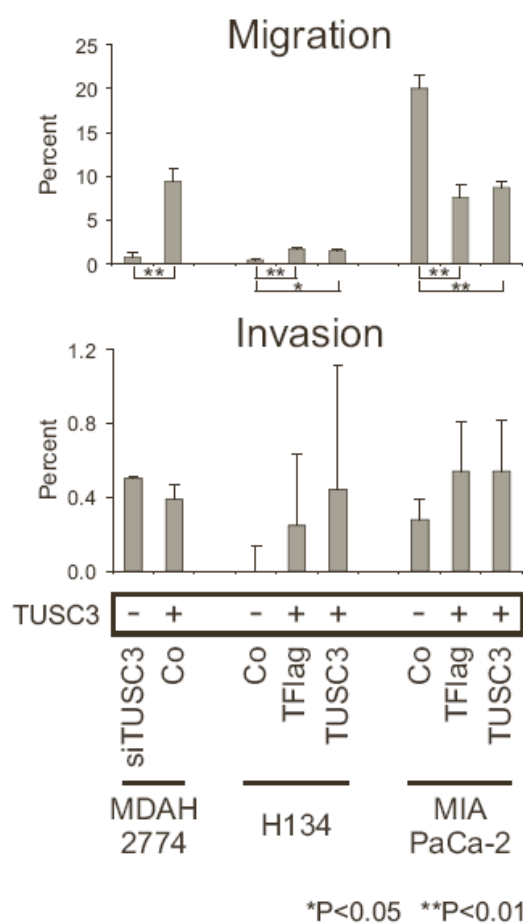


Figure 13 Migration and invasion assay MDAH 2774, H134, MIA PaCa-2, in percent of total cell numbers. Experiments were performed in triplicates, the significance was calculated by the T-test and marked by one (P<0.05) or two asterisks (P<0.01).

Chick chorioallantoic membrane (CAM) Invasion Assay

MDAH 2774

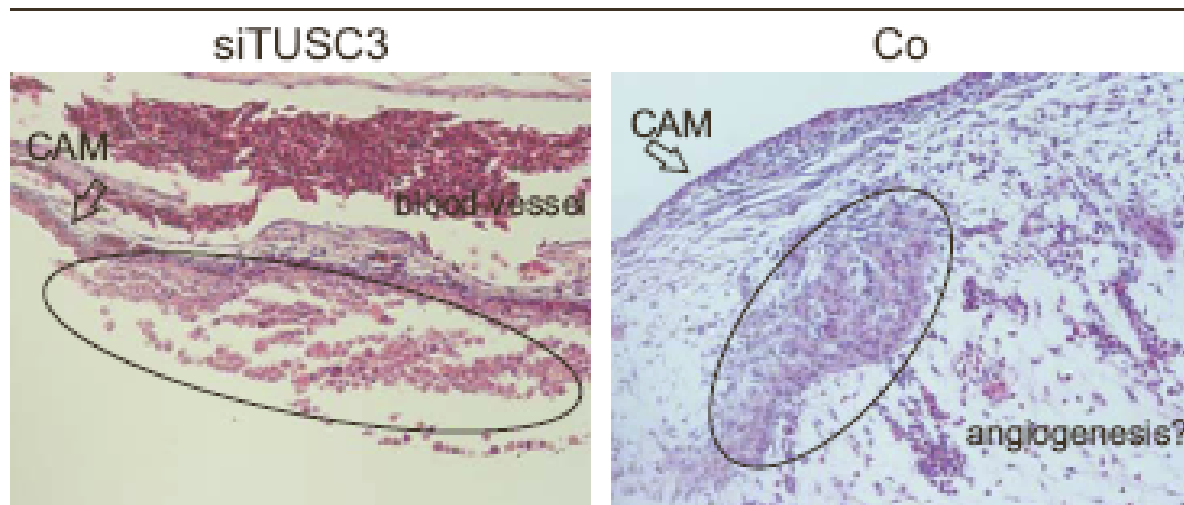


Figure 14 Chick chorioallantoic membrane Invasion Assay (HE stained)

After ten days of growing, the *TUSC3*-positive cells have invaded the tissue through the chorioallantoic membrane, clearly visible in Figure 14. Apparently, the tumor is so prospered, that it begins with angiogenesis. To affirm this finding, there must be performed some more experiments, particularly in variation of time and with other cell lines.

The MDAH siTUSC3 cells seem to be not able to penetrate the membrane. This would be consistent with the observation that metastases of the ovarian cancer grow on the peritoneum without firm attachment.

3.7. Localization of *TUSC3*

Western blot - Sub-cellular fractionation

Since prediction programs for protein localization (PANTHER) diverged substantially for prediction of the subcellular localization of TUSC3 [40], we confirmed the most likely localization by two independent approaches, namely the endoplasmic reticulum (ER) where it forms part of the oligosaccharyltransferase complex. Western blots for the FLAG epitope (probing the TUSC3-FLAG fusion protein) on highly enriched subcellular fractions of H134 cells (microsomes, soluble cytoplasm, mitochondria, lysosomes, and

nuclei) exclusively showed a band in the microsome fraction, comprised of endoplasmic reticulum membranes and minor amounts of the cytoplasmic membrane (Fig. 15).

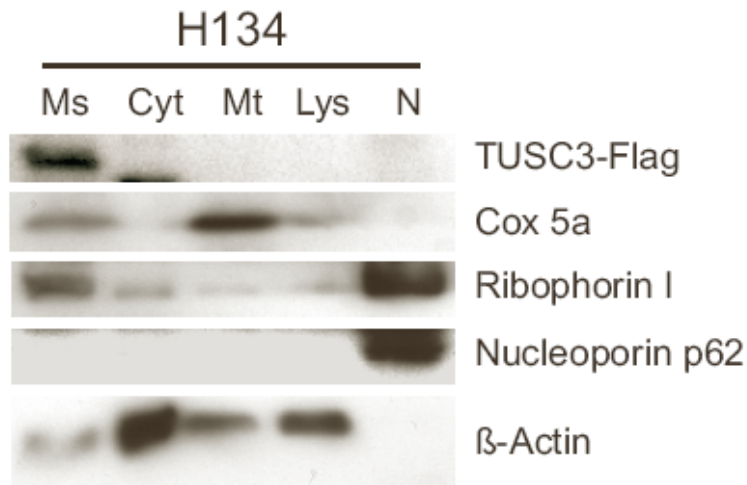


Figure 15 Western blot analysis of subcellular fractions for FLAG-tagged TUSC3 (TUSC3-Flag) in the ovarian cancer cell line H134. Fractions (Ms, microsomes; Cyt, cytoplasm; Mt, mitochondria; Lys, lysosomes; and N, nuclei) were probed with ribophorin I, β-actin, cox 5a, no marker, and nucleoporin p62, respectively.

Immunofluorescence

In addition, an immunofluorescent colocalization experiment revealed a perfect overlap of the of the *TUSC3*-FLAG protein and calnexin, an integral protein of the endoplasmic reticulum used as marker for the ER.

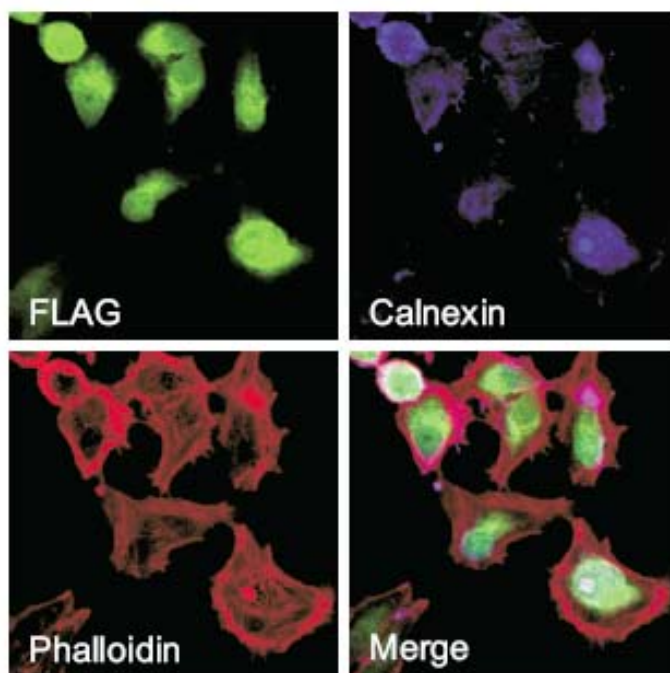


Figure 16 Colocalization experiment on fixed H134 cells stained for the TUSC3-FLAG fusion protein with anti-FLAG, for an integral endoplasmic reticulum protein with anti-calnexin, and with phalloidin as a counterstain.

3.8. Impact on Glycosylation

Having confirmed the localization of TUSC3 in the endoplasmic reticulum, we investigated the putative function of TUSC3 in N-glycosylation by Western blot analysis of integrin $\beta 1$, a well-known example for differential glycosylation with impact on functionality, employing microsome fractions of H134 and MIA PaCa-2 cells. Since MDAH siTUSC3 has only a very weak integrin $\beta 1$ expression an analysis of this cell line model was impracticable. In both cell lines the ratio between fully glycosylated mature and incompletely glycosylated precursor integrin $\beta 1$ increased upon reconstituted *TUSC3* expression (by a factor of 2.0 and 2.6 for H134 and MIA PaCa-2, respectively).

Additionally, a ~ 10 kDa shift towards higher mobility of the mature integrin $\beta 1$ was observed, suggesting a differential (probably decreased) N-glycosylation. As a control, a complete removal of N-glycosylated oligosaccharides was achieved by digestion with PNGase F, resulting in bands of equal mobility at ~ 80 kDa, consistent with the sequence-derived protein mass of roughly 85 kDa (Fig. 17).

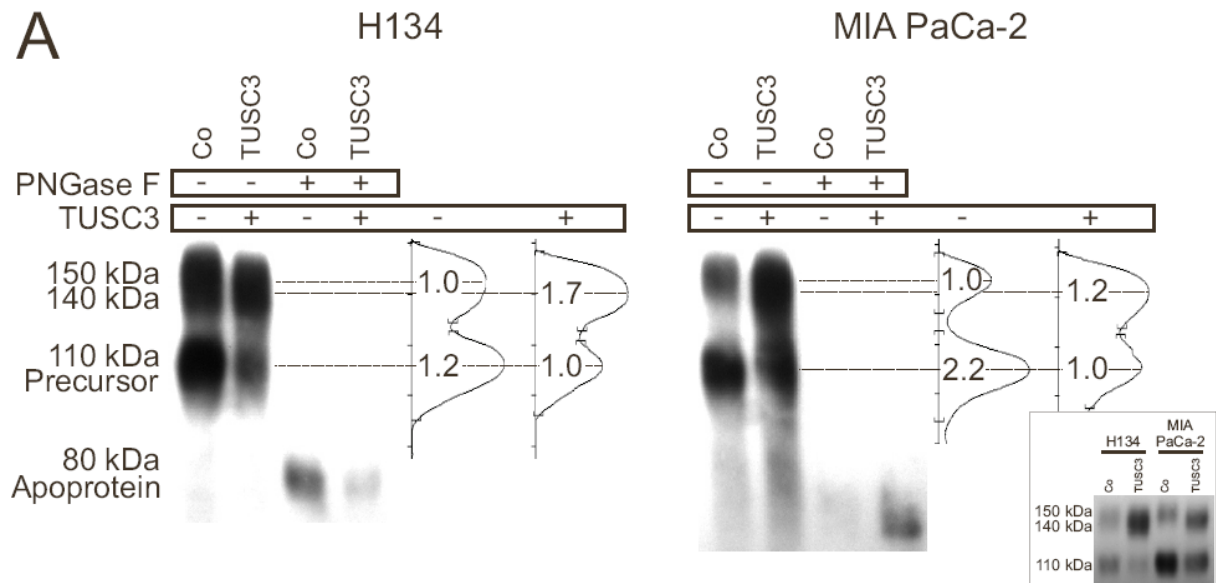


Figure 17 Western blot analysis of integrin $\beta 1$ in H134 and MIA PaCa-2 cell lines. Since MDAH siTUSC3 shows only very weak integrin $\beta 1$ expression an analysis of this cell line model was impracticable. Integrin $\beta 1$ revealed two bands, one at ~110 kDa representing the precursor $\beta 1$ -pool in the ER, and one at ~140-150 kDa representing the mature $\beta 1$ protein. In *TUSC3*-reconstituted cell lines the band representing mature $\beta 1$ showed a ~10 kDa shift towards higher mobility. Treatment of proteins with the deglycosylating enzyme, PNGase F, eliminated the differential mobility and resulted in one band approximately at the position of the calculated apoprotein mass (~80 kDa). Adjacent to the blots, quantification curves are shown. Bands with the smaller values were set to unity for each cell line model. The molecular weight shift and the change of the mature / precursor ratio was more pronounced after a shorter run (inset).

Mobility shifts of mature integrin $\beta 1$ in both directions have already been described previously and were accompanied by changes of sialylation levels regulating the binding affinity to collagen I [41].

An immunocytochemical staining for sialylated proteins using a specific lectin, SNA, revealed a substantial increase of sialylation in *TUSC3*-positive cells compared to *TUSC3*-negative cells. (Fig. 19).

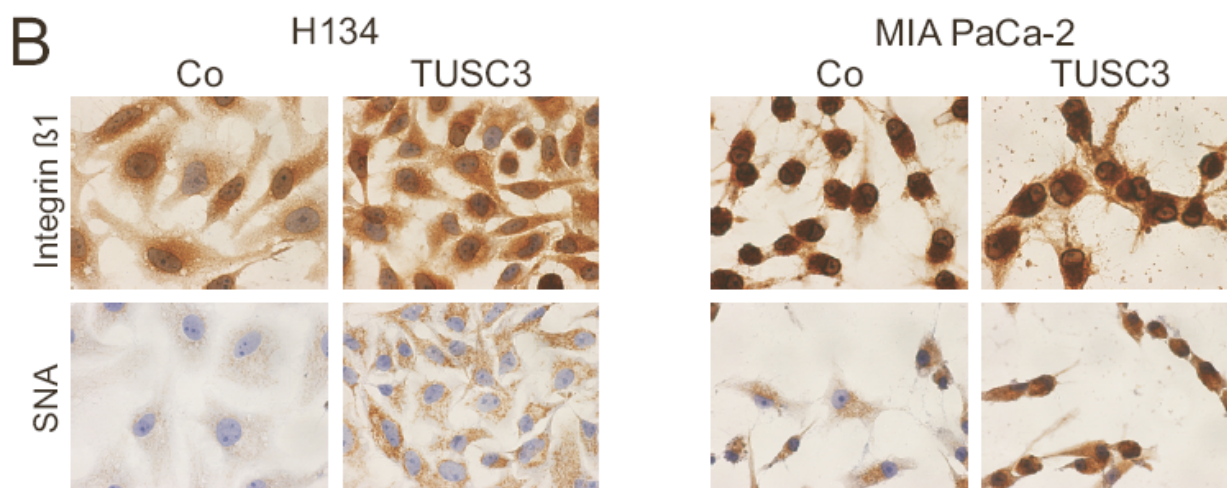


Figure 18 Immunocytochemical stains for integrin $\beta 1$ and sialylated proteins in general (SNA) are shown for the cell line models H134 and MIA PaCa-2. Cell were counterstained with hematoxylin/eosin.

3.9. Adhesion Assay

To assess the impact of the observed glycosylation modifications of integrin $\beta 1$ on collagen I binding in our cell line models, we performed adhesion assays. Although levels of mature integrin $\beta 1$ were reduced in *TUSC3*-negative cells compared to precursor proteins, adhesion to collagen I was significantly increased, whereas adhesion to BSA as a control was unaffected (Fig. 20).

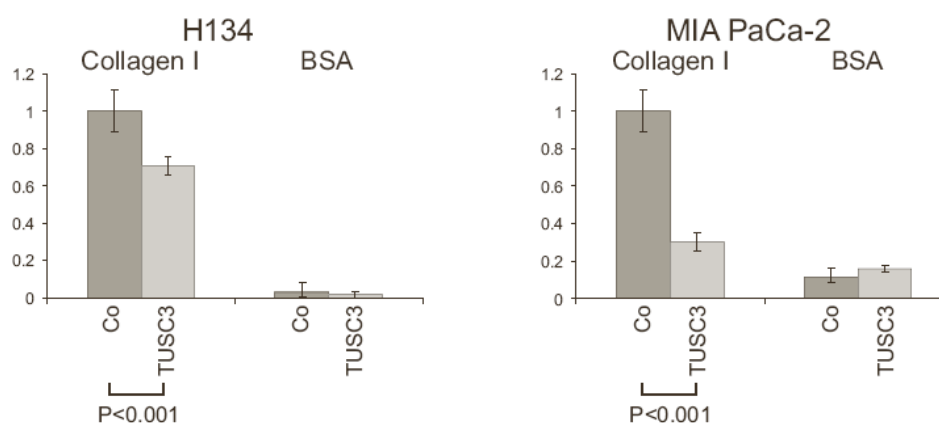


Figure 19 Adhesion of cells to collagen I and BSA (as control) coated 96-well plates were tested in octuples and the significance calculated by T-tests. Binding of the control cells to collagen I was arbitrarily set one.

Adhesion assays with gelatin, fibronectin, laminin, and collagen IV are depicted below. But the differences between the TUSC-negative cell and the control cell line on the BSA-coated control are too high, so the other results are not utilizable (Fig. 21).

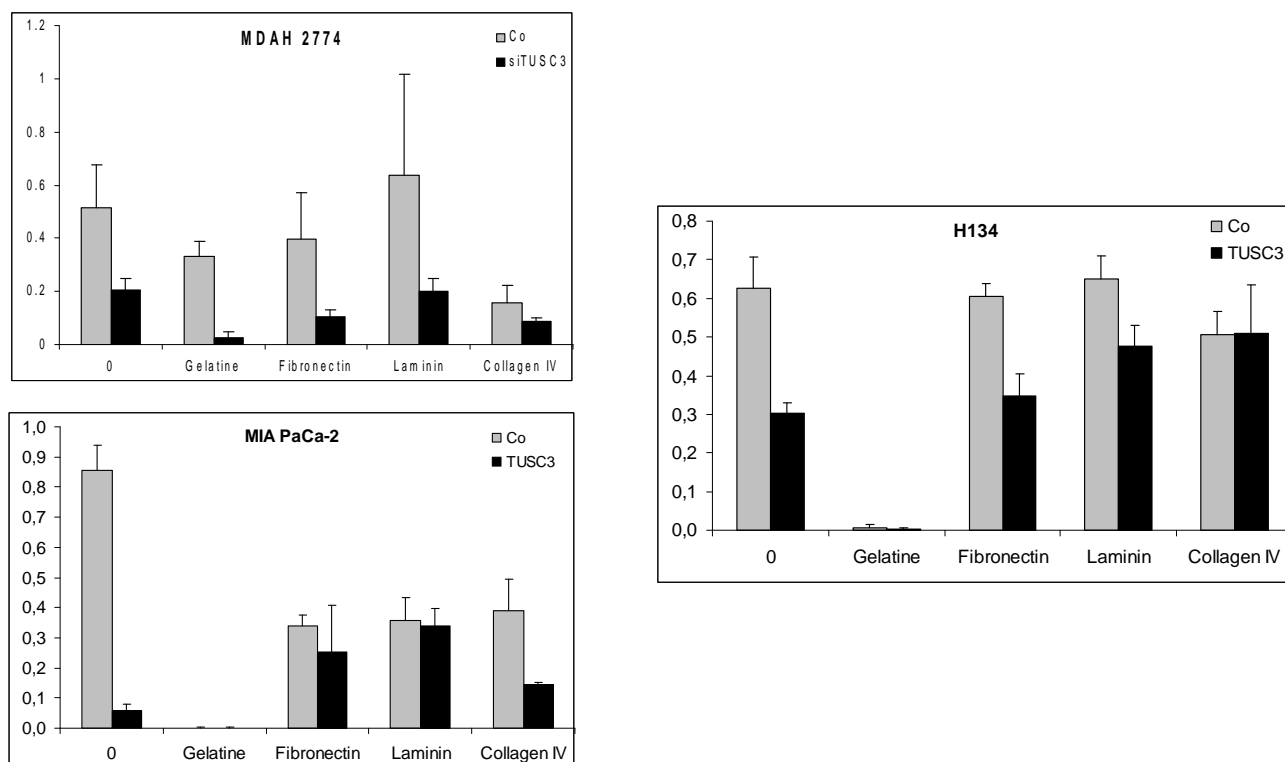


Figure 20 Adhesion assay with gelatin, fibronectin, laminin, and collagen IV

Catterall et al. detected high expression of the highly-glycosylated glycoprotein CD44 on several ovarian tumor lines. It is a receptor for hyaluronic acid (HA) but can also interact with other ligands, such as osteopontin, collagens, and matrix metalloproteinases (MMPs) and so we performed a HA-adhesion assay. HA was found in association with extracellular membranes and sometimes with the cell membrane as a pericellular coat (PC), peritoneal mesothelial cells produce a PC that contains large amounts of HA. Studies have suggested that CD44 could interact in vitro with HA on the mesothelial cells and tumor lines that express CD44 give higher adhesion to mesothelial cells. [42]

Because the bindings of the cells to HA are very weak, standard deviations were very high, but a trend is noticeable, that both MIA PaCa-2 cell lines and MDAH Co have the strongest bond to hyaluronic acid (Fig. 22).

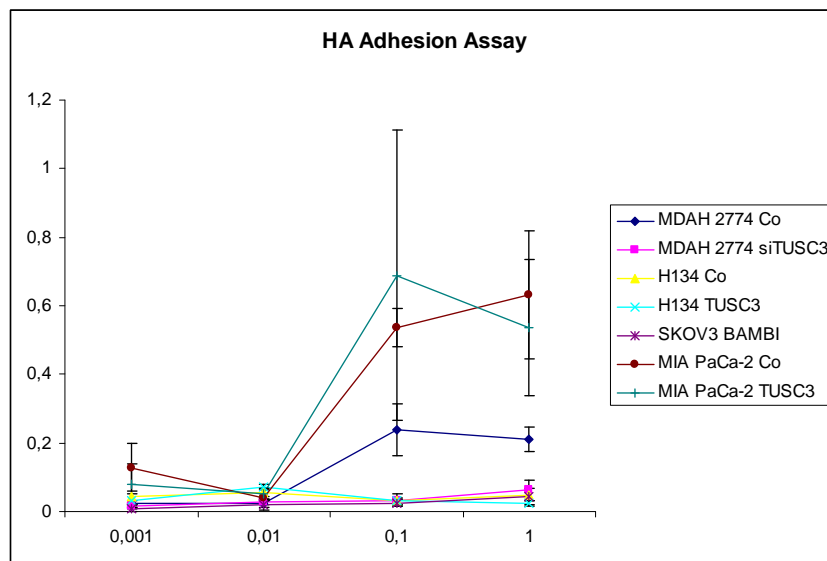


Figure 21 Hyaluronic acid adhesion assay

4. Discussion

4.1. Clinical results and Methylation

TUSC3, originally named *N33*, was first described as a candidate TSG in the mid 1990s, based on the description of three homozygous deletions [25]. Mutational analysis performed in prostate cancer and various other tumor entities failed to reveal a significant rate of protein disruptive mutations and the interest in *TUSC3* consequently vanished.

Using publicly available gene expression profiling data, we have systematically screened for down-regulated genes on 8p22 and identified *TUSC3* as one candidate. A quantitative expression analysis by real-time RT-PCR confirmed the significant down-regulation of *TUSC3* in ovarian cancer tissues and an explorative correlation with clinical parameters showed that patients with reduced *TUSC3* expression at the time of diagnosis seem to have a shortened overall survival [24]. Clinical results showed a significant impact on progression free survival and overall survival of women with ovarian carcinomas with loss or reduction of *TUSC3* expression (Fig. 22).

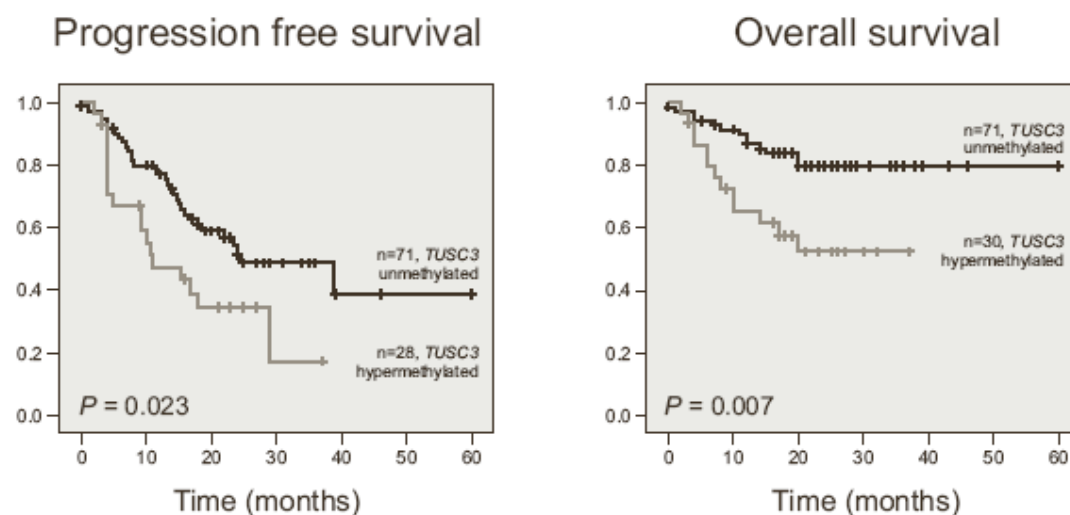


Figure 22 Plots of Kaplan-Meier estimates for progression free and overall survival of patients with tumor samples with hypermethylated or unmethylated *TUSC3*.

A similar result was recently obtained in larynx and pharynx carcinomas, where loss of *N33* (*TUSC3*) was significantly correlated with poor survival [43]. In colorectal cancer LOH frequency of chromosomal band 8p22 was 67%, one of the highest values found in this study, accompanied by significantly reduced expression of *TUSC3* in tumors

compared to normal tissues as well as in tumor samples of paired tumor and normal tissues [44].

4.2. *TUSC3* – *Ostp3*

In 2003 the gene product of *TUSC3* was identified as the human homolog to *S. cerevisiae* Ost3p and it was shown to be weakly associated with the oligosaccharyltransferase complex by co-purification experiments [27]. Oligosaccharyltransferase is an integral membrane protein complex in the endoplasmatic reticulum that catalyzes N-linked glycosylation of secreted and membrane proteins. First, the expected localization in the endoplasmatic reticulum was confirmed by using FLAG-tagged *TUSC3* (western blot: Fig. 15; co-localization by immunofluorescence: Fig. 16). However, the molecular function of *TUSC3* in the human protein complex remains unclear [27], whereas the loss of Ost3p in yeast resulted in biased under-glycosylation of selected acceptor substrates *in vitro* [45].

The glycosylation of proteins and other substrates is involved in numerous biological processes [46] such as cell-cell or cell-matrix interactions which are very important steps in cancerogenesis. Aberrant glycosylation of proteins was found in essentially all types of *in vitro* cancer models and human cancers, and many glycosyl epitopes constitute tumor-associated antigens [30, 41]. Altered glycosylation of tumor cell surface proteins has been observed repeatedly [26] but a long-standing debate is whether aberrant glycosylation is a result or a cause of cancer.

4.3. *In vitro* cell line models

To explore the putative function of *TUSC3* as part of the oligosaccharyltransferase complex in cancer cells we generated three cell line models with either epigenetically silenced (MDAH 2774) or reconstituted *TUSC3* expression (H134 and Mia-PaCa-2) (Fig. 8).

In all three cell line models high *TUSC3* expression correlated significantly with decreased proliferation (Fig. 10), consistent with the significantly better prognosis of patients with *TUSC3*-positive cancers. The clones with lower *TUSC3* expression showed increased proliferation rates and the MDAH si*TUSC3* cell line showed decreased sensitivity to TGF- β -mediated growth inhibition (Fig. 11). Changes in TGF- β signalling are critical events in carcinogenesis and most frequently provided by the insensitivity to its

anti-proliferative effects. Also the rate of apoptosis in the presence of TGF- β was significantly decreased (Fig. 12).

But this was the only parameter which changed reproducibly upon *TUSC3* (re-)expression. Changes in morphology (Fig. 9), migration, and invasion (Fig. 13) were dependent on the origin of the cell line (ovary or pancreas) and this is consistent with the highly cell-line dependent influence of *TUSC3* expression on whole genome expression profiles. But for the ovarian cell lines, there seems to be a trend: cells with high *TUSC3* expression show better ability for migration. Unfortunately, invasion assays in the 24-well plate trans-well system did not bring any clear results. Therefore, we performed a chick CAM invasion assay with the MDAH 2774 cell line. As depicted in Fig. 14, cells with higher *TUSC3* expression invaded through the CAM into the tissue. MDAH si*TUSC3* cells seem to be not able to penetrate the membrane.

4.4. Glycosylation

Glycosylation is an important posttranslational modification that occurs in every cell and has a significant impact on numerous biological processes.

The glycosylation pattern of mature integrin $\beta 1$ and the ratio of mature to precursor protein changed uniformly upon *TUSC3* re-expression in two carcinoma cell lines of different origins (ovary and pancreas). The observed difference in integrin $\beta 1$ glycosylation is known to influence extracellular matrix binding. Furthermore, the amount of sialylated glycoproteins was substantially decreased in both *TUSC3*-negative cell lines (Fig. 19). Therefore, we conclude that *TUSC3* seems to be involved in post-translational maturation (i.e. glycosylation) of integrin $\beta 1$ and probably other glycoproteins. Integrin $\beta 1$ signalling is regulated by extracellular matrix (ECM) binding affecting multiple cellular functions such as proliferation, changes in cytoskeletal organization, motility, and various other processes. Modifications in integrin $\beta 1$ glycosylation is a well confirmed regulatory mechanism for ECM binding and subsequent signalling [35]. Local tumor spread to the peritoneum (trans-coelomic metastasis) is the predominant mechanism of tumor progression in ovarian cancer and the main cause for bad prognosis. It is hypothesized that tumor cell aggregates, so-called spheroids, rather than single cells are responsible for this dissemination. Collagen I is a major component of the mesothelial peritoneum surface and promotes integrin $\beta 1$ -mediated spheroid adhesion and spread [47-50]. Therefore, the significantly increased affinity of *TUSC3*-negative cells to collagen I (Fig. 20), caused by

differential integrin $\beta 1$ glycosylation, provides an intriguingly plain explanation for the strong tumor suppressive function of TUSC3.

Unfortunately, we could not strengthen these results by performing other adhesion assays with gelatin, fibronectin, laminin, and collagen IV: the differences between the TUSC-negative cell and the control cell line on the BSA-coated control are too high, so the other results are not utilizable (Fig. 21). The adhesion assay with hyaluronic acid did not bring another prove neither because the bindings of the cells to HA are very weak, standard deviations were very high. But a trend is noticeable that both MIA PaCa-2 cell lines and MDAH Co have the strongest bond to hyaluronic acid (Fig. 22).

Furthermore, changes of integrin $\beta 1$ glycosylation were shown to affect the migration ability through cytoskeletal rearrangements as indicated by a disorganized actin stress-fibre network [51], which we also observed in our cell line models (Fig. 9).

4.5. Additional clinical Syndroms: Does N33 play a Role in Mental Retardation?

Very recently, supporting data from a distantly related scientific field have been presented on a conference: A frameshift mutation of TUSC3 co-segregated with individuals displaying non-syndromic mental retardation which was diagnosed as a congenital disorder of glycosylation (CDG), disorders characterized by impairment of glycoprotein biosynthesis, but without any direct evidence for impaired glycosylation of target proteins (Molinari et al., Eur J Hum Genet. 15, Suppl. 1, Abstract C38 ; [52]). We are in cooperation with this group and received primary fibroblasts from a patient.

Molinari et al. report that two genes are involved in autosomal and X-linked non-syndromic mental retardation (NSMR). They studied two sibs born to second cousin French parents and presenting NSMR. Via linkage analysis with autozygosity mapping in affected and healthy children and parents, they identified a unique homozygous region on chromosome 8p23.1-p22. The interval encompasses the gene N33/TUSC3 encoding one subunit of the oligosaccharyltransferase (OTase) complex which is an oligomeric membrane protein complex that catalyses the transfer of preassembled high-mannose oligosaccharide onto asparagin residues of nascent polypeptides entering the lumen of the endoplasmatic reticulum, which is the key step of N-glycosylation. [28]

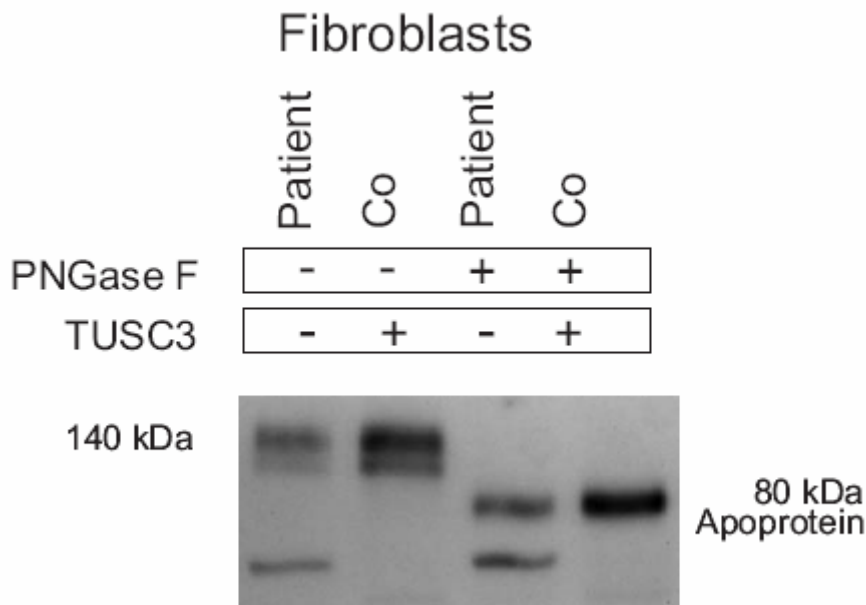


Figure 23 Western blot analysis of integrin $\beta 1$ in fibroblasts

As Molinari et al. describe in their publication, glycosylation analyses of fibroblasts harbouring the *TUSC3* mutation did not reveal any impairment of glycan structures quality nor in their transfer onto nascent proteins. Therefore - to show the glycosylation pattern - we performed the western blot as shown above using the fibroblasts expecting analogue results as with our cell lines H134 and MIA PaCa-2 (Fig. 17): a ~ 10 kDa shift towards higher mobility of the mature integrin $\beta 1$ suggesting a differential (probably decreased) N-glycosylation, maybe because of expression of *TUSC3*. But regrettably, we were unable to prove our expectations. As depicted in figure 23, the bands at the marker of 140 kDa do not show any clear differences in level.

One explanation could be another gene on 8p22 found by Molinari's group, which negatively correlates with *TUSC3*: at least in human fibroblast cells, the gene expression of *IAP* is significantly increased in cells harbouring a *TUSC3* mutation. *IAP* could therefore functionally compensate for the lack of *TUSC3* protein thus resulting in a normal N-glycosylation. [38]

Whatever its detailed function turns out to be, currently *TUSC3* methylation and therefore knock down/silencing is a promising new prognostic marker for ovarian cancer, which should be evaluated prospectively. For a more specific approach for antagonistic therapy targeting integrin $\beta 1$ we traced indications but could not find any clear evidence.

5. References

1. Wachtler, F.H., ed. *Histologie*. 7.A. ed. 2005, Facultas Universitätsverlag. 569.
2. Hanahan, D. and R.A. Weinberg, *The hallmarks of cancer*. Cell, 2000. **100**(1): p. 57-70.
3. Jemal, A., et al., *Cancer statistics, 2005*. CA Cancer J Clin, 2005. **55**(1): p. 10-30.
4. Chien, J.R., et al., *Molecular pathogenesis and therapeutic targets in epithelial ovarian cancer*. J Cell Biochem, 2007. **102**(5): p. 1117-29.
5. Holschneider, C.H. and J.S. Berek, *Ovarian cancer: epidemiology, biology, and prognostic factors*. Semin Surg Oncol, 2000. **19**(1): p. 3-10.
6. Makar, A.P., et al., *Prognostic value of pre- and postoperative serum CA 125 levels in ovarian cancer: new aspects and multivariate analysis*. Obstet Gynecol, 1992. **79**(6): p. 1002-10.
7. Ludwig, J.A. and J.N. Weinstein, *Biomarkers in cancer staging, prognosis and treatment selection*. Nat Rev Cancer, 2005. **5**(11): p. 845-56.
8. Laird, P.W., *The power and the promise of DNA methylation markers*. Nat Rev Cancer, 2003. **3**(4): p. 253-66.
9. Obstetrics, I.F.o.G.a., *Committee on Gynecologic Oncology*. 2007, Dorothy Shaw.
10. Society, A.C., *How is Ovarian Cancer staged?* 2008.
11. Society, A.C., *Ovarian Cancer: Causes, Risk Factors and Prevention*. 2008.
12. Cottreau, C.M., et al., *Endometriosis and its treatment with danazol or lupron in relation to ovarian cancer*. Clin Cancer Res, 2003. **9**(14): p. 5142-4.
13. Rodriguez, C., et al., *Estrogen replacement therapy and ovarian cancer mortality in a large prospective study of US women*. Jama, 2001. **285**(11): p. 1460-5.
14. Murdoch, W.J., *Ovarian surface epithelium, ovulation and carcinogenesis*. Biol Rev Camb Philos Soc, 1996. **71**(4): p. 529-43.
15. Henriksen, R., et al., *Expression and prognostic significance of TGF-beta isoforms, latent TGF-beta 1 binding protein, TGF-beta type I and type II receptors, and endoglin in normal ovary and ovarian neoplasms*. Lab Invest, 1995. **73**(2): p. 213-20.
16. Choi, K.C., et al., *The regulation of apoptosis by activin and transforming growth factor-beta in early neoplastic and tumorigenic ovarian surface epithelium*. J Clin Endocrinol Metab, 2001. **86**(5): p. 2125-35.
17. Berchuck, A., et al., *The role of peptide growth factors in epithelial ovarian cancer*. Obstet Gynecol, 1990. **75**(2): p. 255-62.
18. Higashi, T., et al., *Overexpression of latent transforming growth factor-beta 1 (TGF-beta 1) binding protein 1 (LTBP-1) in association with TGF-beta 1 in ovarian carcinoma*. Jpn J Cancer Res, 2001. **92**(5): p. 506-15.
19. Akhurst, R.J. and R. Derynck, *TGF-beta signaling in cancer--a double-edged sword*. Trends Cell Biol, 2001. **11**(11): p. S44-51.
20. Auersperg, N., et al., *Characterization of cultured human ovarian surface epithelial cells: phenotypic plasticity and premalignant changes*. Lab Invest, 1994. **71**(4): p. 510-8.
21. Fujimoto, J., et al., *Expression of E-cadherin and alpha- and beta-catenin mRNAs in ovarian cancers*. Cancer Lett, 1997. **115**(2): p. 207-12.
22. Aunoble, B., et al., *Major oncogenes and tumor suppressor genes involved in epithelial ovarian cancer (review)*. Int J Oncol, 2000. **16**(3): p. 567-76.

23. Brown, M.R., et al., *Allelic loss on chromosome arm 8p: analysis of sporadic epithelial ovarian tumors*. Gynecol Oncol, 1999. **74**(1): p. 98-102.
24. Pils, D., et al., *Five genes from chromosomal band 8p22 are significantly down-regulated in ovarian carcinoma: N33 and EFA6R have a potential impact on overall survival*. Cancer, 2005. **104**(11): p. 2417-29.
25. Bova, G.S., et al., *Physical mapping of chromosome 8p22 markers and their homozygous deletion in a metastatic prostate cancer*. Genomics, 1996. **35**(1): p. 46-54.
26. MacGrogan, D., et al., *Structure and methylation-associated silencing of a gene within a homozygously deleted region of human chromosome band 8p22*. Genomics, 1996. **35**(1): p. 55-65.
27. Kelleher, D.J., et al., *Oligosaccharyltransferase isoforms that contain different catalytic STT3 subunits have distinct enzymatic properties*. Mol Cell, 2003. **12**(1): p. 101-11.
28. Kelleher, D.J. and R. Gilmore, *An evolving view of the eukaryotic oligosaccharyltransferase*. Glycobiology, 2006. **16**(4): p. 47R-62R.
29. Dennis, J.W., M. Granovsky, and C.E. Warren, *Glycoprotein glycosylation and cancer progression*. Biochim Biophys Acta, 1999. **1473**(1): p. 21-34.
30. Kobata, A. and J. Amano, *Altered glycosylation of proteins produced by malignant cells, and application for the diagnosis and immunotherapy of tumours*. Immunol Cell Biol, 2005. **83**(4): p. 429-39.
31. Collard, J.G., et al., *Cell surface sialic acid and the invasive and metastatic potential of T-cell hybridomas*. Cancer Res, 1986. **46**(7): p. 3521-7.
32. Dennis, J.W., et al., *Beta 1-6 branching of Asn-linked oligosaccharides is directly associated with metastasis*. Science, 1987. **236**(4801): p. 582-5.
33. Kakugawa, Y., et al., *Up-regulation of plasma membrane-associated ganglioside sialidase (Neu3) in human colon cancer and its involvement in apoptosis suppression*. Proc Natl Acad Sci U S A, 2002. **99**(16): p. 10718-23.
34. Lau, K.S., et al., *Complex N-glycan number and degree of branching cooperate to regulate cell proliferation and differentiation*. Cell, 2007. **129**(1): p. 123-34.
35. Seales, E.C., et al., *Ras oncogene directs expression of a differentially sialylated, functionally altered beta1 integrin*. Oncogene, 2003. **22**(46): p. 7137-45.
36. Varki, A., *Essentials of glycobiology*. 1999, Cold Spring Harbor, NY: Cold Spring Harbor Laboratory Press [Bethesda Md. : National Center for Biotechnology Information].
37. Eklund, E.A. and H.H. Freeze, *The congenital disorders of glycosylation: a multifaceted group of syndromes*. NeuroRx, 2006. **3**(2): p. 254-63.
38. Molinari, F., P.S. Foulquier, and L. Colleaux, *Oligosaccharyltransferase subunits mutations in non-syndromic mental retardation*. submitted, 2008.
39. Kunzi-Rapp, K., et al., *Chorioallantoic membrane assay: vascularized 3-dimensional cell culture system for human prostate cancer cells as an animal substitute model*. J Urol, 2001. **166**(4): p. 1502-7.
40. Pils, D., et al., *Methylation of N33 (TUSC3) Alters N-Glycosylation Patterns and Predicts Independent Ovarian Cancer Patient Outcomes*. submitted, 2008.
41. Hakomori, S., *Glycosylation defining cancer malignancy: new wine in an old bottle*. Proc Natl Acad Sci U S A, 2002. **99**(16): p. 10231-3.
42. Catterall, J.B., et al., *Binding of ovarian cancer cells to immobilized hyaluronic acid*. Glycoconj J, 1997. **14**(7): p. 867-9.

43. Guervos, M.A., et al., *Deletions of N33, STK11 and TP53 are involved in the development of lymph node metastasis in larynx and pharynx carcinomas*. Cell Oncol, 2007. **29**(4): p. 327-34.
44. Andersen, C.L., et al., *Frequent occurrence of uniparental disomy in colorectal cancer*. Carcinogenesis, 2007. **28**(1): p. 38-48.
45. Karaoglu, D., D.J. Kelleher, and R. Gilmore, *Functional characterization of Ost3p. Loss of the 34-kD subunit of the Saccharomyces cerevisiae oligosaccharyltransferase results in biased underglycosylation of acceptor substrates*. J Cell Biol, 1995. **130**(3): p. 567-77.
46. Varki, A., *Biological roles of oligosaccharides: All of the theories are correct*. Glycobiology, 1993. **3**: p. 97-130.
47. Lessan, K., et al., *CD44 and beta1 integrin mediate ovarian carcinoma cell adhesion to peritoneal mesothelial cells*. Am J Pathol, 1999. **154**(5): p. 1525-37.
48. Burleson, K.M., L.K. Hansen, and A.P. Skubitz, *Ovarian carcinoma spheroids disaggregate on type I collagen and invade live human mesothelial cell monolayers*. Clin Exp Metastasis, 2004. **21**(8): p. 685-97.
49. Burleson, K.M., et al., *Ovarian carcinoma ascites spheroids adhere to extracellular matrix components and mesothelial cell monolayers*. Gynecol Oncol, 2004. **93**(1): p. 170-81.
50. Burleson, K.M., et al., *Disaggregation and invasion of ovarian carcinoma ascites spheroids*. J Transl Med, 2006. **4**: p. 6.
51. Guo, H.B., et al., *Aberrant N-glycosylation of beta1 integrin causes reduced alpha5beta1 integrin clustering and stimulates cell migration*. Cancer Res, 2002. **62**(23): p. 6837-45.
52. Molinari, F., et al., *Oligosaccharyltransferase subunits mutations in non-syndromic mental retardation*. submitted, 2008.

6. Abbreviations

GS	Growth Signal
PDGF	Platelet-derived Growth Factor
TGF α/β	Transforming Growth Factor
TNF α	Tumor Necrose Factor
EGF-R	Epidermal Growth Factor - Receptor
IGF	Insulin-like-Growth Factor
FGF	Fibroblast Growth Factor
HER2	human Epidermal Growth Factor Receptor 2
Bcl-2	B-cell Lymphoma 2
Bak	Bcl-2 homologous Antagonist Killer
ALT	Alternative Lengthening of Telomeres
VEGF	Vascular Endothelial Growth Factor
MMP	Matrix Metalloproteinase
CA	Cancer Antigen
TSG	Tumor Suppressor Gene
LMP	Low Malignant Potential
EOC	Epithelial Ovarian Cancer
FIGO	International Federation of Gynecology and Obstetrics
AJCC	American Joint Committee on Cancer
LOH	Loss of Heterozygosity
BRCA1	Breast Cancer 1 (a TSG)
OSE	Ovarian Surface Epithelium
EMT	Epithelial to mesenchymal Transition
MET	Mesenchymal to epithelial Transition
EDACC	Epigenomics Data Analysis and Coordination Center
ATCC	American Type Culture Collection
OTase	Oligosaccharyltransferase complex
Ost3	Gamma subunit of the oligosaccharyltransferase complex of the ER lumen
NSMR	non-syndromic Mental Retardation
CDG	Congenital Disorders of Glycosylation
qrt PCR	quantitative real time Polymerase Chain Reaction

PBS	Phosphate buffered Saline
FCS	Fetal Calf Serum
siRNA	small interfering RNA
PVDF	Polyvinylidenfluorid
SDS	Sodium Dodecyl Sulfate
ECL	Emitting Chemoluminescence
HRP	Horseradish peroxidase
FITC	Fluorescein Isothiocyanate
PI	Propidiumiodid
FACS	Fluorescence Activated Cell Sorting
ELISA	Enzyme Linked Immunosorbent Assay
HA	Hyaluronic acid
BSA	Bovine Serum Albumin
CAM	Chorioallantoic membrane
SNA	Sambucus nigra Agglutinin
bp	base pares

Curriculum vitae

Personal information

Surname / First name Gugerell Alfred
Address Barnabitengasse 3/16, 1060 Vienna, Austria
Date of Birth 09.01.1982
Nationality Austria

Education

Date January 2007 to March 2008
Principal subjects Diploma thesis at the Department of Internal Medicine I,
Division Oncology, Prof. Krainer
Name / type of organization Medical University of Vienna; A-1090

Date 11.7.2006 to 11.8.2006
Principal subjects Individual laboratory at the Univ. Clinic of Blood Serology
and Transfusion Medicine, Prof. Dr. Panzer
Name / type of organization Medical University of Vienna; A-1090

Date June 2006
Principal subjects Archaeological work at historical graves at Sensengasse 1-3,
A-1090
Name / type of organization MA 7 – Kultur, Referat Stadtarchäologie, Friedrich
Schmidt-Platz 5, A-1082 Vienna

Date since September 2001
Principal subjects Study of Biology, branch of study: Anthropology (since July
2004)
Name / type of organization University of Vienna; A-1010

Date September 1992 to June 2000
Title of qualification awarded "Reifeprüfung" (general qualification for university
entrance, school-leaving examination)
Principal subjects Humanistic grammar school
Name / type of organization Gymnasium Sachsenbrunn, private grammar school of the
Archdiocese Vienna; A-2880

Date September 1988 to June 1992
Principal subjects Elementary school
Name / type of organization Volksschule Aspang-Markt, A-2870